WAVE INTERACTIONS OF H-TYPE

FLOATING BREAKWATER

By

NOR NADIA AIDA BINTI MAHADI

Supervisor: Dr Teh Hee Min

Civil Engineering Department

Wave Interactions of H-Type Floating Breakwater

by

Nor Nadia Aida Binti Mahadi

Dissertation submitted in partial fulfillment of
the requirements for the
Bachelor of Engineering (Hons)
(Civil Engineering)

SEPTEMBER 2013

Universiti Teknologi PETRONAS
Bandar Seri Iskandar
31750 Tronoh
Perak Darul Ridzuan

CERTIFICATION OF APPROVAL

Wave Interactions of H-Type Floating Breakwater

By

Nor Nadia Aida Binti Mahadi

A project dissertation submitted to the
Civil Engineering Department
of Universiti Teknologi PETRONAS
in partial fulfillment of the requirement for the
BACHELOR OF ENGINEERING (Hons)
(CIVIL ENGINEERING)

Approved by,

_____

(Dr. Teh Hee Min)

UNIVERSITI TEKNOLOGI PETRONAS

TRONOH, PERAK

September 2013

CERTIFICATION OF ORIGINALITY

This is to certify that I am responsible for the work submitted in this project, that the original work is my own except as specified in the references and acknowledgements, and that the original work contained herein have not been undertaken or done by unspecified sources or persons.

_____

NOR NADIA AIDA BINTI MAHADI

ABSTRACT

Rapid development along coastal area calls for protection structures to be built along the coastline to protect the area from destructive wave energy. However, suppression of wave energy itself has been a challenge to many coastal engineers and researchers worldwide. Numerous studies and countless efforts were put into the development of hard and soft strategies in protecting coastal infrastructures. Breakwaters are one of such method, generally constructed to protect a certain area by breaking the incoming waves and dissipating the energy to a harmless level. Breakwaters are widely implemented due to high degree of protection offered. However despite its excellent wave dampening ability, fixed breakwaters are getting negative views with regards to the environment, i.e. interruption of sediment transport, interference with fish migration, water pollution and downdrift erosions. Floating breakwaters are introduced as an alternative to the fixed breakwater with regards to environmental and cost advantage. H-type floating breakwater is a new configuration of floating breakwater that was recently proposed and developed. This study is conducted to further evaluate the performance of H-type floating breakwater as well as the effects of draft on its performance. A medium size test model with a scale of 1:10 was constructed using plywood and coated by fiberglass for waterproofing. This model was tested in a 25 meter wave flume against random waves to simulate realistic sea conditions. The variable parameters of this study include wave period, wave steepness and breakwater draft. The performance of the H-type floating breakwater was assessed based on the reflection and transmission coefficients as well as energy dissipation. The results were compared against other breakwater models as well as the larger scale of similar H-type model configuration. Conclusively, the H-type breakwater model with scale of 1:10 is an effective floating breakwater with excellent capability in attenuating wave energy by energy dissipation and wave reflection.

ACKNOWLEDGEMENT

The authoress would like to express her sincere gratitude to the supervisor, Dr. Teh Hee Min; lecturer of Civil Engineering Department, Universiti Teknologi PETRONAS for his guidance throughout this project. Thank you for the continuous supports and motivation.

To the authoress' laboratory partner; Mr Muhammad Syahmi Maarof Bin Azizan who has been conducting the experiments together with the authoress, the authoress would like to extend special appreciation and gratitude for helping along the whole duration of the study as well as for the motivational and emotional support.

Special appreciation is given to the postgraduate students; Miss Nur Zaidah and Miss Noor Diyana for their guidance in preparing and conducting of the experiments as well as in analyzing the experimental results

A heartfelt appreciation is extended to the Offshore Laboratory technicians and staffs, particularly Mr. Meor Asnawan, Mr Iskandar and Mr. Mohd Zaid for their assistance to the authoress throughout the whole duration of the study. This study would have been a failure without their constant help in solving problems and errors faced by the authoress during the experiments.

An earnest appreciation to Universiti Teknologi PETRONAS for the opportunity given to conduct a research study for the authoress' final year project. The authoress had received an opportune chance in meeting many wonderful people along the way of completing this project.

To my family, thank you for your prayers and moral support. And last but not least, millions of thanks to the lecturers, technicians and friends who have been contributing for this project.

Thank you.

NOR NADIA AIDA BINTI MAHADI

Civil Engineering Department

TABLE OF CONTENT

SYMBOLS

H_i	incident wave height
H_r	reflected wave height
H_t	transmitted wave height
C_R	reflection coefficient
C_T	transmission coefficient
C_L	energy loss coefficient
C_L^2	energy loss
E_i	incident wave energy
E_r	reflected wave energy
E_t	transmitted wave energy
E_l	energy loss
L	wavelength
T	wave period
f	frequency
B	width of breakwater
h	height of breakwater
l	length of breakwater
D	draft of breakwater
d	water depth
B/L	relative breakwater width
H_i/L_p	incident wave steepness
H_i/gT^2	wave steepness parameter
D/d	breakwater draft-to-water depth ratio

LIST OF FIGURES

LIST OF TABLES

CHAPTER 1

INTRODUCTION

1.1 BACKGROUND STUDY

Breakwaters are man-made structures that are placed near the coastlines as barriers to protect harbors or shore from destructive wave energy. It reduces the wave force through dissipation of wave height and speed by breaking the wave formation.

Various designs of breakwaters have been studied in the past decade. The most conventional breakwaters have been the rubble-mound breakwaters that are made of stones. Fixed breakwaters offer excellent storm protection and higher durability in withstanding the destructive waves; however they contribute several environmental drawbacks such as being immovable and trapping debris and sediments in its vicinity. The fixed breakwaters may not be economically and environmentally friendly, as the cost and materials increase exponentially with water depth.

Floating breakwaters are considered as an alternate method of wave suppression as they are more economically feasible compared to fixed breakwaters. Floating breakwaters offer advantages in terms of transportation and cost, while being reusable and removable. The cost of floating breakwaters is insensitive to water depth and the breakwaters can be easily moved to serve a new location with minimum effort, however they are not as strong as its counterpart. The performance of floating breakwaters is dependent on the mooring system used and it gives varying effects on wave suppression. Table 1.1 shows the summarized advantages and disadvantages of both fixed and floating breakwaters.

Table 1.1: Advantages and disadvantages of fixed and floating breakwaters

	Advantages	Disadvantages
Fixed Breakwater	• Protection from high and long-period waves • Dislocated stones and rubbles can be easily repaired • Habitat for aquatic life	• Semi-permanent structure • High construction cost • Sensitive to water depth • Aesthetically displeasing
Floating Breakwater	• Easily moved / arranged • Appropriate where fixed breakwaters are unfeasible • Insensitive to water depth • Low installation cost • No interference with water flow • Aesthetically pleasing	• Ineffective against high or long-period waves • Subjected to failure in heavy storms • High repair cost

A number of researches were conducted experimentally and numerically to investigate the roles of breakwater and wave characteristics in producing stronger and more reliable design of floating breakwaters. The box-type floating breakwater has been the most widely studied structure, which became the motivation for the development of the H-type floating breakwater (Teh and Nuzul, 2013) as shown in Figure 1.1. The new design of H-type floating breakwater offer promising results in attenuating wave energy when compared to most floating breakwater designs, however the tests and experiments conducted were limited and further experiments are required to attest to the performance of the design.

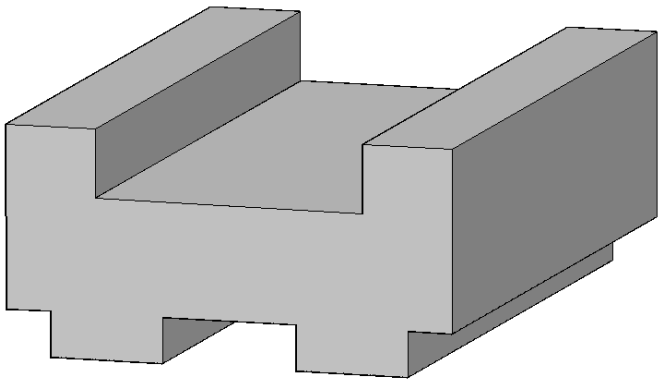

Figure 1.1: The H-type floating breakwater model

1.2 PROBLEM STATEMENT

Floating breakwaters are protective structures developed to protect coastal areas from destructive energy of waves. New designs of breakwaters are developed through thorough studies and experimenting. The ideal experiment is carried out in a place with similar setting as the targeted location. However the lack of appropriate facility and the high expense of prototype fabrication makes it impossible to conduct an experiment and testing on the capabilities of breakwaters out in the open sea. Therefore all coastal-related experiments are conducted in laboratories using physical modeling of smaller scales due to inadequate facilities and budget constraint. The efficiency tests of H-type floating breakwater were done using small-scale models of 1:5 and 1:20 ratios; however the results may be subjected to several drawbacks:

1) Draft effect

   The draft of models in previous studies (Dexter, 2013) was affected by tension in mooring lines and could not be properly studied.

2) Test limitations

   Due to facility and budget constraints, the models were subjected to small test cases such as small range of wave period and limited water depth and breakwater drafts.

3) Inadequate measurement techniques

   The incident and reflected waves were measured by a moving probe method, which were subjected to instrumental and human errors.

4) Scale effects

   Possible varying observations might have occurred due to disproportional relevant forces between the prototype and the models.

This study was conducted using a medium size of H-type breakwater model with a scale of 1:10 with the intent to assess the effects of draft and the performance of breakwater in various wave conditions.

1.3 SIGNIFICANCE OF STUDY

Developments along the coastal area are increasing rapidly each year due to high economic and social demands. This situation calls for protection structures to be built along the coastline to reduce risks. Fixed breakwater is generally the standard solution to providing protection, however the economic standing in Malaysia requires for inexpensive measure, which rules out fixed breakwater as the major mean of coastal protection. Instead, floating breakwater is considered as a feasible alternative in regards of cheaper expense with more or less similar degree of performance.

Continuous development of floating breakwaters by researchers and engineers worldwide for improved breakwater design with higher performance and better efficiency drives for the new development of H-type floating breakwater. The significance of this study is to establish the performance of H-type breakwater design in comparison to other existing floating breakwaters.

1.4 OBJECTIVES OF STUDY

The objectives of this study are as follows:

i) To evaluate the effects of drafts in the performance of H-type floating breakwater in attenuating wave energy;
ii) To test the performance of H-type floating breakwater against wider range of wave conditions; and
iii) To compare the performance of H-type floating breakwater against other existing floating breakwaters.

1.5 SCOPE OF STUDY

The scopes of this study are outlined as follows:

i) Literature Review

A comprehensive and thorough study on the related subjects (i.e. wave interactions, floating breakwater models, etc) was carried out.

ii) Model Fabrication

Fabrication of the H-type floating breakwater model to a scale of 1:10

iii) Laboratory Set-up

All test equipments were checked in terms of capabilities and status. The equipments were calibrated prior to testing.

iv) Experiments

Extensive laboratory tests were conducted in the wave flume to assess the hydraulic performance of H-type floating breakwater.

v) Analysis of results

The experimental results obtained from model 1:10 were analyzed to obtain reflected wave heights and spectral wave energy. Comparisons with other floating breakwaters were made.

CHAPTER 2

LITERATURE REVIEW

This chapter outlines general wave interactions of a floating breakwater and the parameters needed in quantifying reflected and transmitted wave heights plus energy dissipation. An introduction on other types of floating breakwaters is included along with the study on scale effects associated to physical modeling.

2.1 WAVE INTERACTIONS

During storm events, the incident waves carry high amount of energy towards the shoreline. When confronted by coastal structures like breakwaters, the waves may undergo one or several forms of interactions; i.e. wave run-up, wave overtopping, wave reflection, wave transmission, wave breaking and wave dissipation as shown in Figure 2.1.

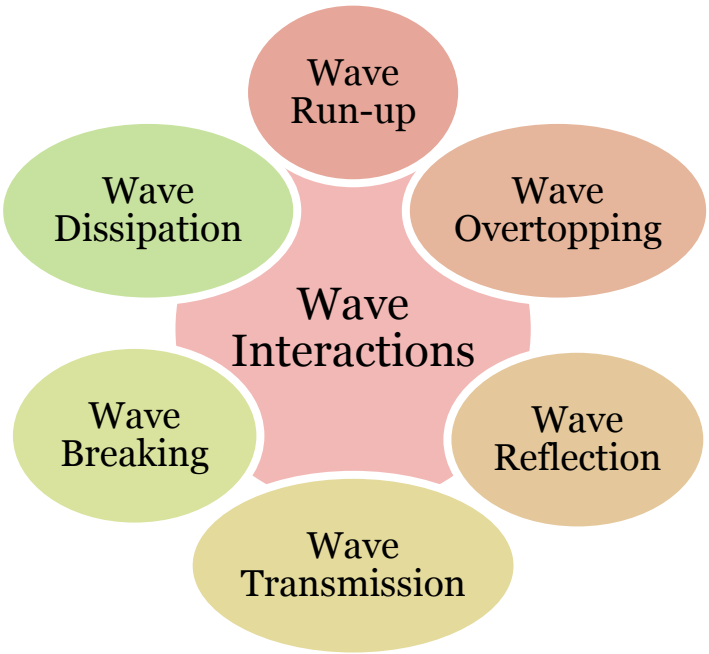

Figure 2.1: Wave interactions

2.1.1 WAVE BREAKING

Xie (2013) stated that wave breaking plays an important role in wave-structure interactions and is highly responsible for wave energy dissipation mechanism as well as the generation of turbulence, vortices and near shore currents in the surf zone. Wave breaking occurs when the wave steepness increases to a critical point, usually when the water depth is approximately equal to wave height. The waves may break in several different ways; i.e. spilling, plunging, collapsing, and surging as shown in Figure 2.2. The type of wave breaking is dependent on the wave characteristics and the slope of the near shore seabed. Steep waves on mild slopes are inclined to break by spilling water gently from the crests with little reflection of the incident wave energy, whereas long, low waves on steep slopes tend to stay intact and surged up and down the slope instead, with most of the wave energy being reflected (Hedges, n.d.). Breaking waves impose higher amount of forces on structures when compared to equivalent non-breaking waves.

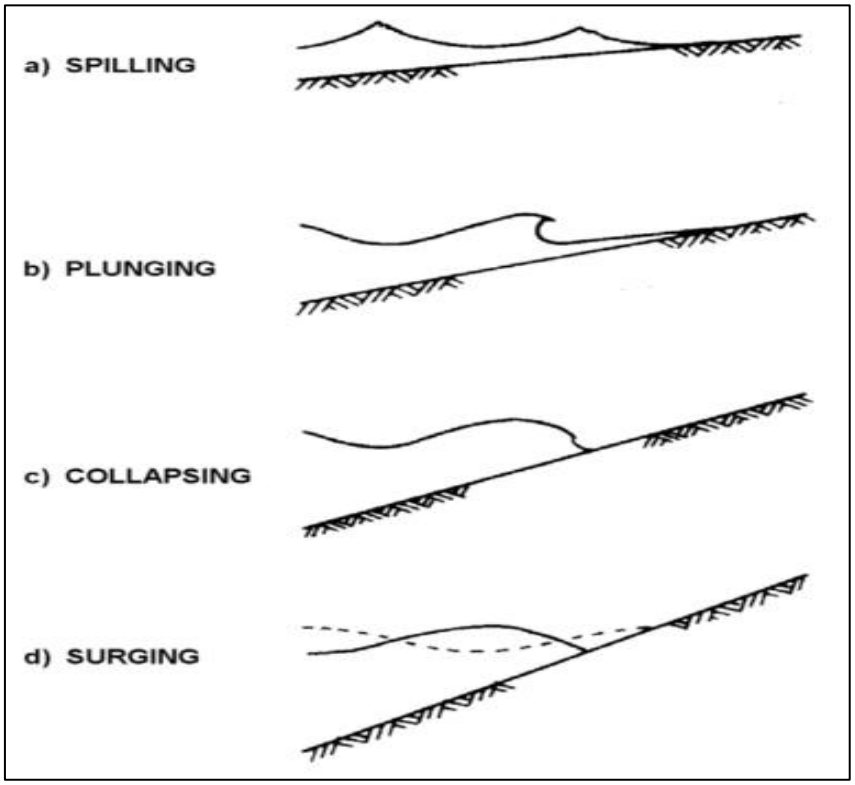

Figure 2.2: Types of wave breaking (Hedges, n.d.)

2.1.2 WAVE RUN-UP

Wave run-up is the upper limit of wave up-rush from wave action on a shore barrier above the still water level (Kobayashi, 1997) as shown in Figure 2.3. The extent of run-up can vary greatly from wave to wave depending on the wave characteristics, shape and slope of near shore.

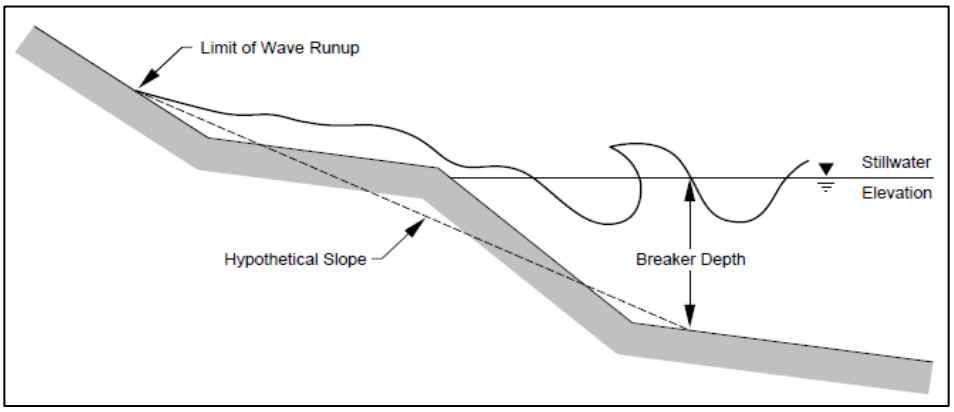

Figure 2.3: Wave run-up sketch (Guidelines and Specifications for Flood Hazard Mapping Partners, 2007)

2.1.3 WAVE OVERTOPPING

Wave overtopping is the process of water overflowing the crest of coastal structures (Geeraerts et al., 2007). When the wave run-up reaches beyond the crest level of coastal structures as shown in Figure 2.4, the waves bypass and overtops the structure. Therefore the prediction of maximum wave run-up is necessary in determining the crest height of the structure required to avoid wave overtopping.

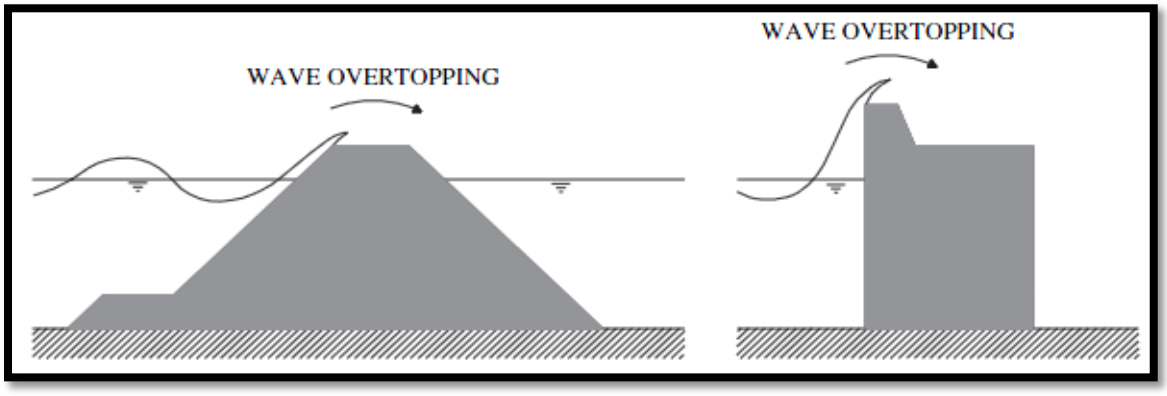

Figure 2.4: Wave overtopping (Geeraerts et al., 2007)

2.1.4 WAVE REFLECTION

Reflection of wave is the re-direction of non-dissipated wave energy by the shoreline or coastal structures to the sea (Chakrabarti, 1999). Reflection is highly apparent when the waves hit on solid seawalls and are reflected back seawards, virtually unaffected by the incoming waves. The reflection coefficient C_r shows the percentage of reflected waves by the obstruction or structures as shown by:

$$C_r = \frac{H_r}{H_i} \tag{2.1}$$

where,

C_r is reflection coefficient,

H_r is reflected wave height, and

H_i is the incident wave height.

Total reflection of wave energy without any energy dissipation is plausible if the obstruction is a smooth, impermeable and solid vertical wall of infinite height, in which case the C_r obtained would be equal to 1. Generally, the coefficient will be less than 0.9 or 90%, and even less for permeable and rough obstructions surfaces.

2.1.5 WAVE TRANSMISSION

Chakrabarti (1999) mentioned that the effectiveness of breakwaters in attenuating the wave energy can be determined from the amount of wave energy transmitted beyond the structure. The breakwater is considered to be effective if the transmission coefficient is small, since it shows that the amount of energy that has transmitted past the structure is much less than the energy level of incident wave. The higher the wave transmission coefficient, the less will be the attenuation of wave energy.

Wave transmission coefficient C_t can be calculated using the following formula:

$$C_t = \frac{H_t}{H_i} \quad (2.2)$$

where,

C_t is transmission coefficient,

H_t is transmitted wave height (leeward side of the structure), and

H_i is the incident wave height (seaward side of the structure).

2.1.6 ENERGY LOSS

When a wave hits an obstacle or a structure, the wave energy will break down into several portions. The first portion of energy will be reflected back seaward of the structure as reflected waves, whereas the second portion includes the transmitted energy that managed to pass through the structure as transmitted waves. The remaining energy is considered as loss energy. The energy transforms into heat, sound and motion upon hitting the structure. The amount of energy loss or energy loss coefficient for a typical flow can be calculated using the following formulas:

$$E_i = E_r + E_t + E_l \quad (2.3)$$

where,

E_i is incident wave energy,

E_r is reflected wave energy,

E_t is transmitted wave energy, and

E_l is energy loss.

$$E = \frac{(pgH)^2}{8} \quad (2.4)$$

Substituting Eq. (2.4) into Eq. (2.3):

$$\frac{(pgH)^2\ i}{8} = \frac{(pgH)^2\ r}{8} + \frac{(pgH)^2\ t}{8} + \frac{(pgH)^2\ l}{8} \qquad (2.5)$$

Simplification:

$$H_i{}^2 = H_r{}^2 + H_t{}^2 + H_l{}^2 \qquad (2.6)$$

Dividing Eq. (2.6) by $H_i{}^2$:

$$1 = C_r{}^2 + C_t{}^2 + C_l{}^2 \qquad (2.7)$$

where,

C_r is reflection coefficient,

C_t is transmission coefficient, and

C_l is energy loss coefficient.

Rearranging Eq. (2.7) will yield:

Energy Loss - $$C_l{}^2 = 1 - (C_t)^2 - (C_r)^2 \qquad (2.8)$$

2.2 RANDOM WAVES

Random waves are made up of a large number of regular wave planes. Random waves do not have a constant wavelength, constant water level elevation but instead it has a random wave phase. When the waves are recorded, a non-repeating wave profile can be seen and the wave surface recorded will be irregular and random. From the profile, some of the individual waves can be identified but overall the wave profile will show significant changes in height and period from wave to wave as shown in Figure 2.5. The spectral method and the wave-by-wave analysis are used to study random waves. Spectral approaches are based on Fourier Transform of the water waves. In wave-by-wave analysis, historic periods of water waves are used and statistical records are developed.

3

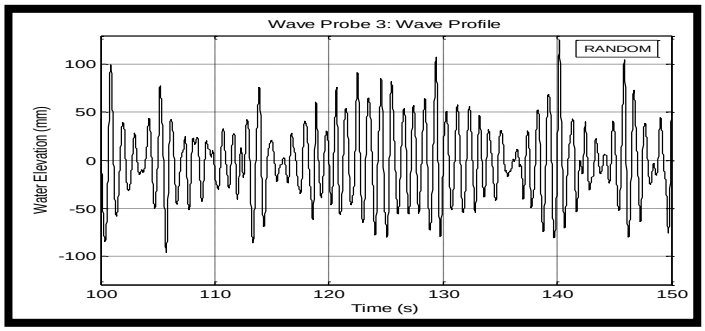

Figure 2.5: Random wave train

2.3 EXISTING FLOATING BREAKWATER MODELS

A number of floating breakwaters have been developed and tested by different researchers in the past. Hales (1981) reviewed five concepts of floating breakwater which includes the pontoon, sloping floats, scrap tires, cylinders, and tethered float. He suggested that the designs of floating breakwaters should be kept as simple, durable and maintenance free as possible; avoiding highly complex structures that are difficult and expensive to design, construct and maintain. Later on, McCartney (1985) introduced four types of floating breakwater including box, pontoon, mat, and tethered float.

A brief description of four types of floating breakwater; box, pontoon, mat, and tethered float is followed by examples of configurations as shown in Figure 2.6.

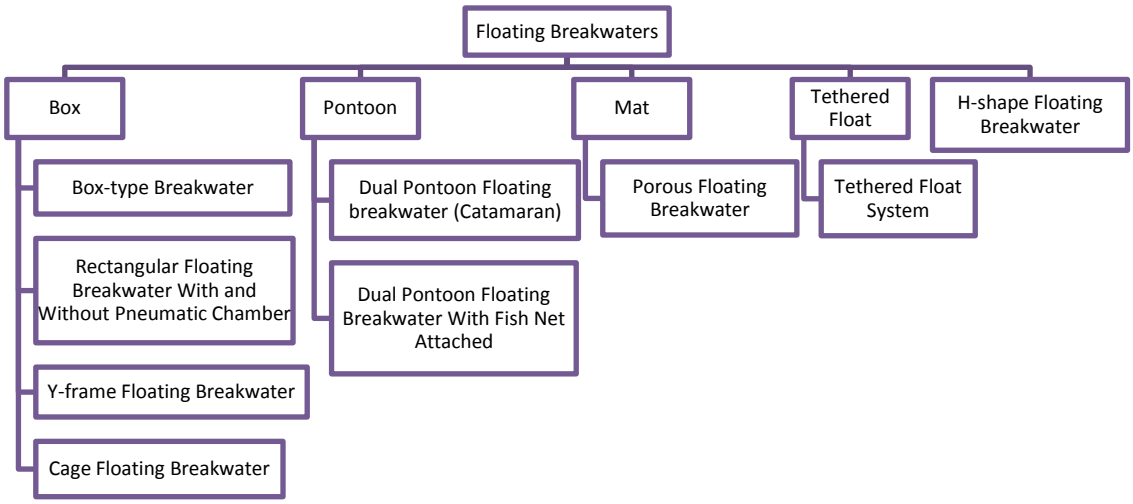

Figure 2.6: Various configurations of floating breakwater

2.3.1 BOX TYPE FLOATING BREAKWATER

This type of breakwater is commonly used due to its simple configuration. It is constructed from reinforced concrete modules which has a density lower than that of sea water with either a solid or hollow body. The floating module is then moored to the sea floor with flexible or tensioned connectors. The common shapes of box type floating are square, rectangle and trapezoidal shape.

2.3.1.1 BOX FLOATING BREAKWATER

McCartney (1985) introduced the box floating breakwater which was constructed of reinforced concrete module. It is commonly rectangular in shape as shown in Figure 2.7. The modules have either flexible connections or are pre- or post-tensioned to make them act as a single unit. It is effective in moderate wave climate.

Figure 2.7: Solid rectangular box-type floating breakwater (McCartney, 1985)

2.3.1.2 RECTANGULAR FLOATING BREAKWATER WITH AND WITHOUT PNEUMATIC CHAMBER

He *et al*. (2011) studied the performance of rectangular shaped breakwaters with and without pneumatic chambers installed on them. He *et al*. (2011) proposed a novel configuration of a pneumatic floating breakwater for combined wave protection and potential wave energy capturing. Pneumatic system uses compressed air trapped in a chamber to produce mechanical motion similarly like a vacuum pump. The development of the concept originates from the oscillating water column (OWC) device commonly used in wave energy utilization (Falcao, 2010). The configuration consists of the box-type breakwater with a rectangular cross section as the base structure, with pneumatic chambers (OWC units) installed on both front and back sides of the box-type breakwater without modifying the geometry of the original base structure as shown in Figure 2.8.

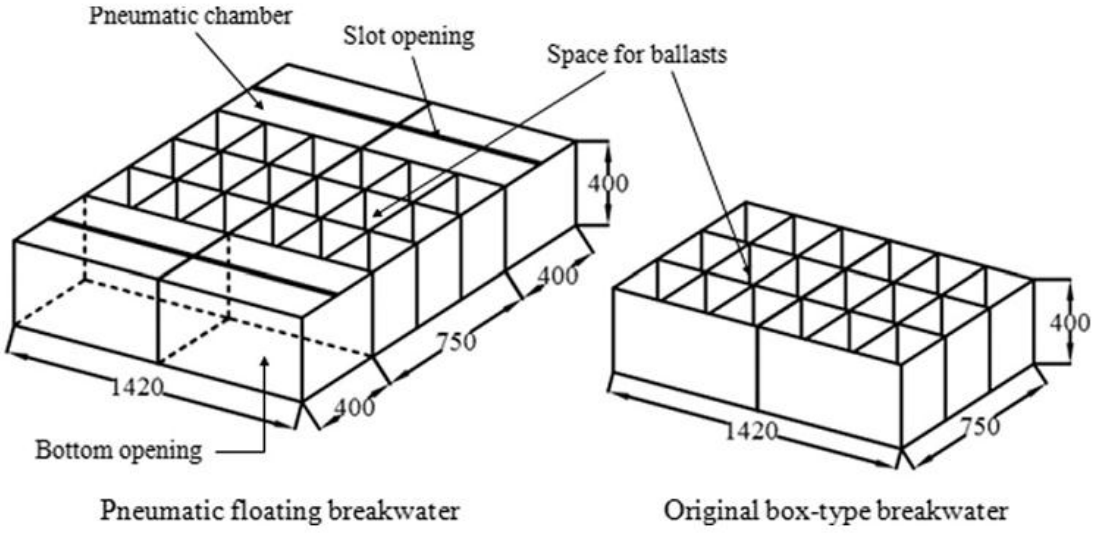

Figure 2.8: Pneumatic floating breakwater and box-type rectangular (He et al., 2011)

2.3.1.3 Y-FRAME FLOATING BREAKWATER

Mani (1991) studied different types of existing breakwaters performance in reducing transmission coefficient. It was suggested that *B/L* ratio should be greater than 0.3 to obtain transmission coefficient below 0.5. Increment of width will cause the construction of the breakwater to increase and handling and installation of the

breakwater will be increasingly difficult. Y-Frame floating breakwater was designed to reduce the width of the floating breakwater by changing its shape as shown in Figure 2.9 without incurring significant extra costs while improving the performance of the breakwater in reduction of the transmission coefficient.

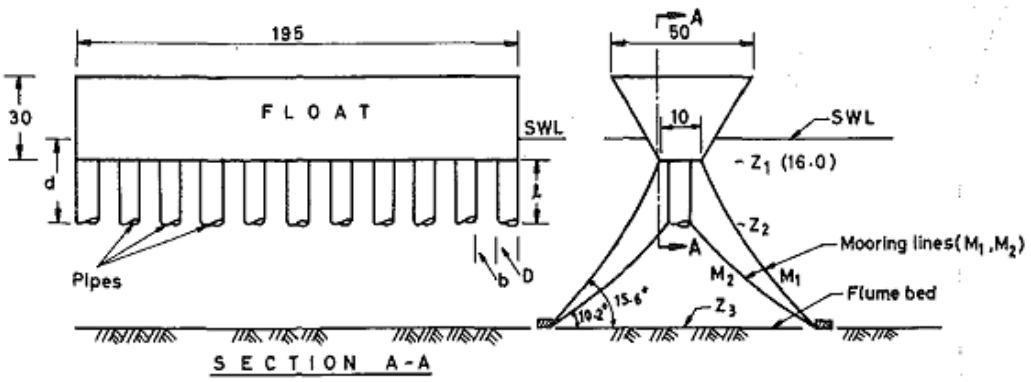

Figure 2.9: Details of the Y-frame floating breakwater (Mani, 1991)

2.3.1.4 CAGE FLOATING BREAKWATER

Murali and Mani (1997) adopted the cost-effective Y-frame floating breakwater (Mani, 1991) in designing the cage floating breakwater which comprises of two trapezoidal pontoons connected together by a nylon mesh with two rows of closely spaced pipes as shown in Figure 2.10. The breakwater offer advantages such as easy on-land fabrication, quick installation, less maintenance cost, and environmental friendly.

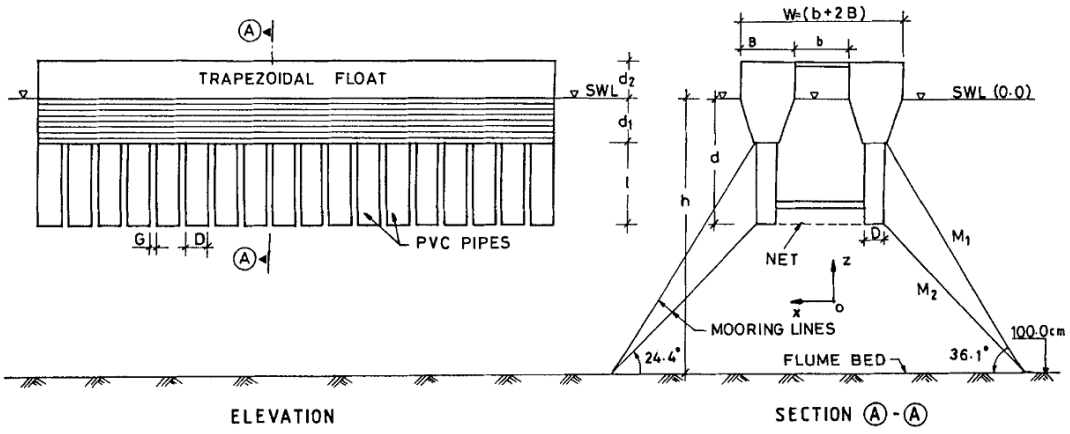

Figure 2.10: Cage floating breakwater (Murali and Mani, 1997)

2.3.2 PONTOON TYPE FLOATING BREAKWATER

Pontoon type floating breakwater (also called Alaska or ladder type) takes on the design of the catamaran used by fishermen in the past as the structure is very stable and rigid. It comprises of two units of rectangular or box shaped breakwaters connected together by a plate or a wooden deck. This structure offers a great option if increasing the draft of a structure is permitted. The width and spacing between the pontoons can be increased so as to offer double protection against waves. The pontoons are made of reinforced concrete embedded with light buoyant materials akin to polystyrene.

2.3.2.1 DUAL PONTOON FLOATING BREAKWATER (CATAMARAN)

Williams and Abul-Azm (1995) investigated the hydrodynamic properties of a dual pontoon breakwater consisting of a pair of floating cylinders of rectangular sections connected by a rigid deck as shown in Figure 2.11. The effects of various waves and structural parameters on the efficiency of the breakwater as a wave barrier were studied. A boundary element technique was utilized to calculate the wave transmission and reflection characteristics.

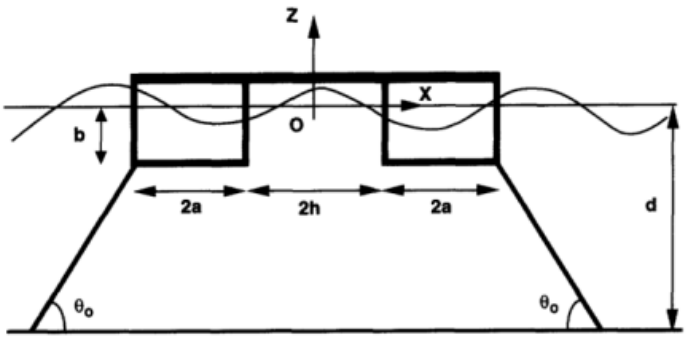

Figure 2.11: Dual pontoon breakwater sketch (Williams and Abul-Azm, 1995)

2.3.2.2 DUAL PONTOON FLOATING BREAKWATER WITH FISH NET ATTACHED

Tang *et al*. (2010) investigated the dynamic properties of a dual pontoon floating structure (DPFS) with and without a fish net attached as shown in Figure 2.12 by using physical and numerical models. The purpose of attaching the fish net is to increase the draft of the structure while at the same time offering a space for marine aquaculture.

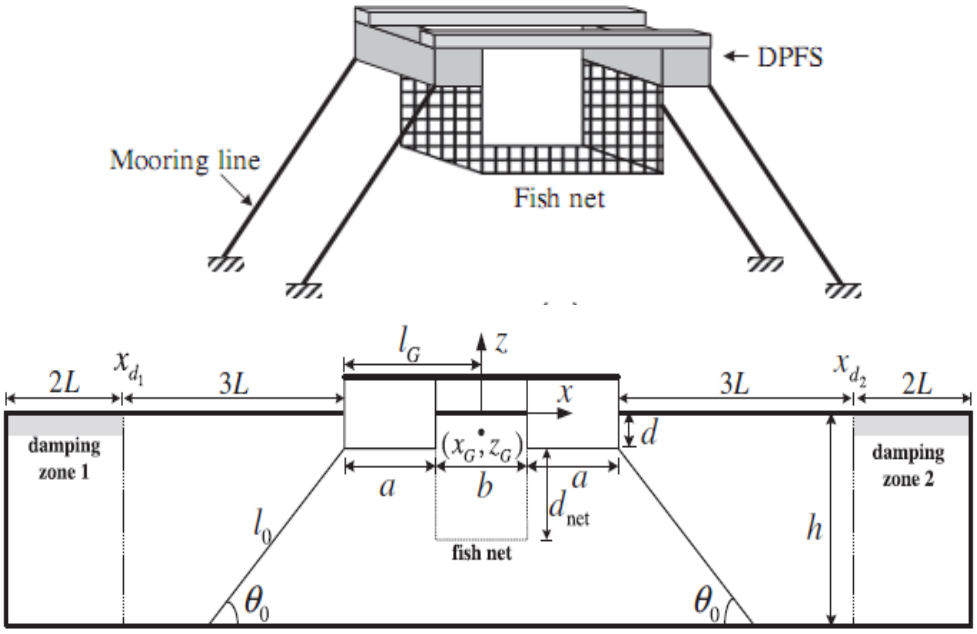

Figure 2.12: Dual pontoon floating breakwater with fish net attached (Tang et al., 2010)

2.3.3 MAT TYPE FLOATING BREAKWATER

Mat type floating breakwater consists of a series of scrap tires or log rafts chained by a cable together and moored to the sea floor. Rubber tires floats well in water and the arrangement of the tires provide a semi-permeable surface which allows some wave energy to be reflected while the other half passed through the configuration and gets dissipated. Floating mat type breakwater offer disadvantages such as lack of buoyancy and unwanted marine growth and silt or debris accumulation in the tires that can sink the breakwater. The main reason for the implementation of this type of breakwater is due to low material and labor cost.

2.3.3.1 POROUS FLOATING BREAKWATER

Wang and Sun (2009) developed a mat-type floating breakwater that consists of a large number of diamond-shaped blocks that was arranged to reduce transmitted wave height as showed in Figure 2.13. They also considered two different mooring models; directional mooring and bidirectional mooring as shown in Figure 2.14 and Figure 2.15 respectively.

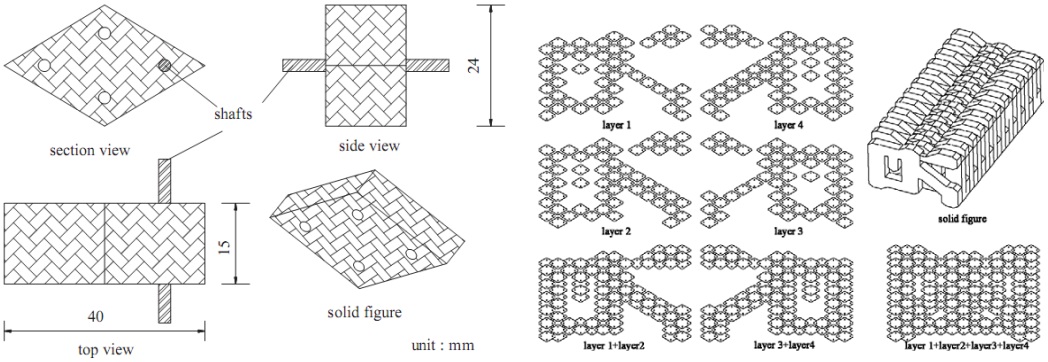

Figure 2.13: Sketch of diamond shape block (left) and arrangement of the blocks (right) (Wang and Sun, 2009)

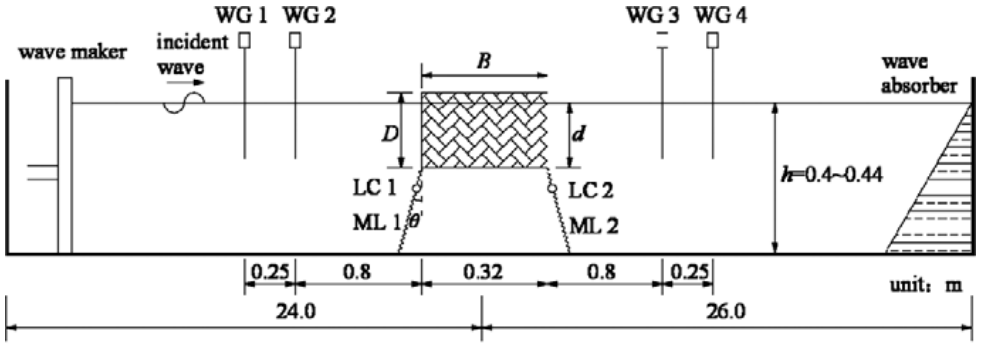

Figure 2.14: Experimental set-up with directional mooring (Wang and Sun, 2009)

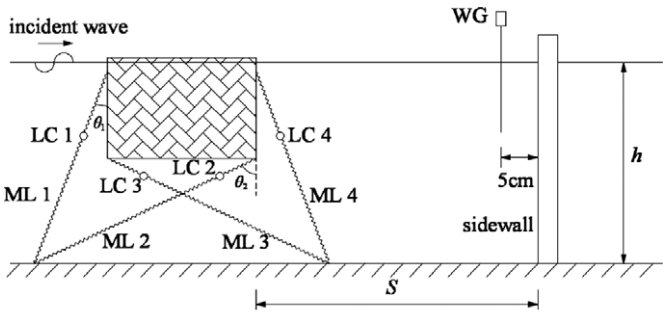

Figure 2.15: Bidirectional mooring (Wang and Sun, 2009)

2.3.4 TETHERED FLOAT TYPE FLOATING BREAKWATER

Tethered type breakwaters are often made up of spherical floats or steel drums with ballasts that are individually tethered to a rigid submerged frame. It is suitable for application in small fishing villages where the waves are not as violent. The size of float needs to be reduced for better performance if it is to be applied in a deeper water region (Vethamony *et al*., 1993).

2.3.4.1 TETHERED FLOAT SYSTEM

Vethamony (1994) studied the wave attenuation characteristics of a tethered float system as shown in Figure 2.16, with respect to wave heights, wave periods, wave depths, depths of submergence of float and float size. The smaller the float size, the higher will be the wave attenuation, since small floats undergo maximum excursion and interfere with the orbital motion of the fluid particles.

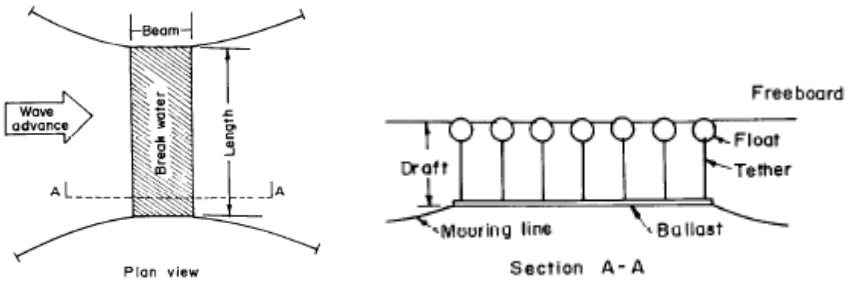

Figure 2.16: Tethered float breakwater (Vethamony, 1994)

2.3.5 H-SHAPE FLOATING BREAKWATER

Teh and Nuzul (2013) studied the hydraulic performance of a newly developed H-shape floating breakwater as shown in Figure 2.17 for regular waves. The aim of this study was to determine the wave transmission, reflection and energy dissipation characteristics of the breakwater model under various wave conditions. The breakwater was previously developed by a group of UTP students for their Engineering Team Project back in 2004. The breakwater was designed to reduce wave energy through reflection, wave breaking, friction and turbulence. The two

"arms" at the top of the main body was designed to facilitate wave breaking at the structure; whereas the two "legs" at the bottom was intended to enhance the weight of the breakwater barrier against wave actions. The breakwater model was made of autoclaved lightweight concrete (ALC) with fiberglass coating. According to Teh and Nuzul (2013), wave transmission coefficient, C_T, decreases with increasing relative breakwater width, *B/L*.

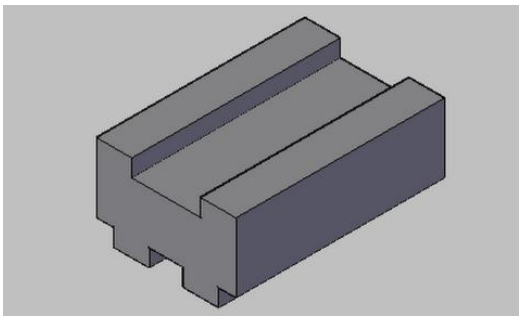

Figure 2.17: H-shape floating breakwater (Teh and Nuzul, 2013)

2.4 PHYSICAL MODELING DOWNSCALING ERRORS

A physical model is a tool for experimenting that represents the real-world prototype in a smaller scale. The down-scaling of the prototype leads to several aspects that can lead to an error in the results. There are basically three effects that may occur from the down-scaling, i.e. model effects, scale effects and measurement effects.

Model effects originate from inaccurate replication of the prototype features such as the geometry of 2D modeling and reflections, flow or wave generation techniques or fluid properties (Hughes, 1993). Model effects may arise if freshwater is used instead of the seawater as the fluid properties are fairly different. Similarly the turbulence intensity level in approach flow or linear wave approximation must be scaled down accordingly. Schüttrumpf and Oumeraci (2005) mentioned that the measurement effects stem from different usage of measurement techniques for data sampling in both model and prototype, for example varying probe sizes and measuring systems. The difference in the techniques will undoubtedly contribute to some errors in the final result.

Scale effects occur when the relevant force ratios are disproportional between model and its real-world prototype which will result in deviations between the up-scaled model and prototype observations (Heller, 2011). While model and measurement effects can be avoided when the modeling and experimentations are done properly, scale effects are considered impossible to circumvent from, as it is extremely difficult to produce perfect miniature model and environmental setting based of the prototype's location. Scale effects will be further explained in the subsequent sections.

2.5 FACTORS AFFECTING SCALE EFFECTS

Scale effects appear in physical modeling because the ratios of relevant forces that are present in the prototype cannot be maintained in a scaled model (Tirindelli et al., 2000). For example, the gravitational force that acts on the prototype cannot be reduced according to the scale ratio; the gravitational force that will act on the model will still be of the same value. Scale effects also comprises of several other factors like the properties of seawater and freshwater, surface tension, air content, viscosity and friction as well as the varying scaling rules, i.e. Froude number, Reynolds numbers, Weber number and Cauchy number.

2.5.1 PROPERTIES OF SEAWATER

Floating breakwaters that are placed along the coastal areas are surrounded by seawater; hence it makes perfect sense for experiments concerning breakwaters and other ocean or coastal engineering subjects to use seawater as the experimental fluid. Unfortunately the acidic properties of the seawater can be damaging to the equipments, in addition to the impracticality of retrieving and transporting the required amount of seawater to the facilities each time the experiment is being carried out. All of these factors lead to the change of experimental fluid to that of freshwater as freshwater can be acquired and replaced easily. Freshwater is also considered as the most practical alternative to seawater, with the assumption that the properties of both liquids are similar. Seawater is normally only about 2.5% more dense, 7.5% more viscous and is 1% higher in surface tension than freshwater at 20°C (Blenkinsopp and Chaplin, 2011).

The assumption is proven to be wrong when several different researchers had found varying results between bubble plumes generated in both freshwater and seawater. The slight difference in the properties of both liquids plays a major role in producing varying outcomes. The knowledge on the relation between the differences and the final outcomes are required to validate small-scale experiments in the laboratories that conduct tests designed to reproduce oceanic processes.

Blenkinsopp and Chaplin (2011) highlighted that the most commonly observed difference in the testing of freshwater and seawater is the bubble size distribution. There are many different results and thoughts on this subject matter, with different groups of researchers presenting supporting evidence to their findings. One group of researchers presented evidence which demonstrates that smaller, sub-millimeter bubbles are present in seawater compared to freshwater. It is popularly believed that the bubble coalescence of freshwater is higher than seawater; hence freshwater have a higher percentage of large bubbles whereas higher number of small bubbles are present in seawater. However, conflicting evidences on the matter was presented by Wu (2000) and Loewen et al. (1996), in which they stated that there are no significant differences between bubbles formed in either freshwater nor seawater.

Blenkinsopp and Chaplin (2011) also reported that similar disagreement was found on void fraction distribution study and total volume air entrained in freshwater and seawater. Chanson et al. (2006) concluded that void fraction with identical flow conditions are smaller in seawater, while Wu (2000) realised that the saltwater which has higher air entrainment will have a larger volume of trapped air than freshwater. The confusion deepens further when Loewen et al. (1996) stated that the formations of bubble flumes are similar in both liquids.

Blenkinsopp and Chaplin (2011) conducted an experiment on void fraction of freshwater, artificial seawater and natural seawater and produced the bubble plume evolution as shown in Figure 2.18. The results has proven that despite having only slight differences in properties, freshwater as an alternative of seawater for a small-scale experiment will still produce a varying result. The strong ionic presence in seawater has a stronger hold on the bubbles as compared to the weak ionic presence in freshwater. Scott (1975) demonstrated that bubbles in seawater are stabilized by the presence of salts once they have reached the surface, and thus persist for a longer period of time, whereas bubbles in freshwater bursts rapidly after reaching the water surface.

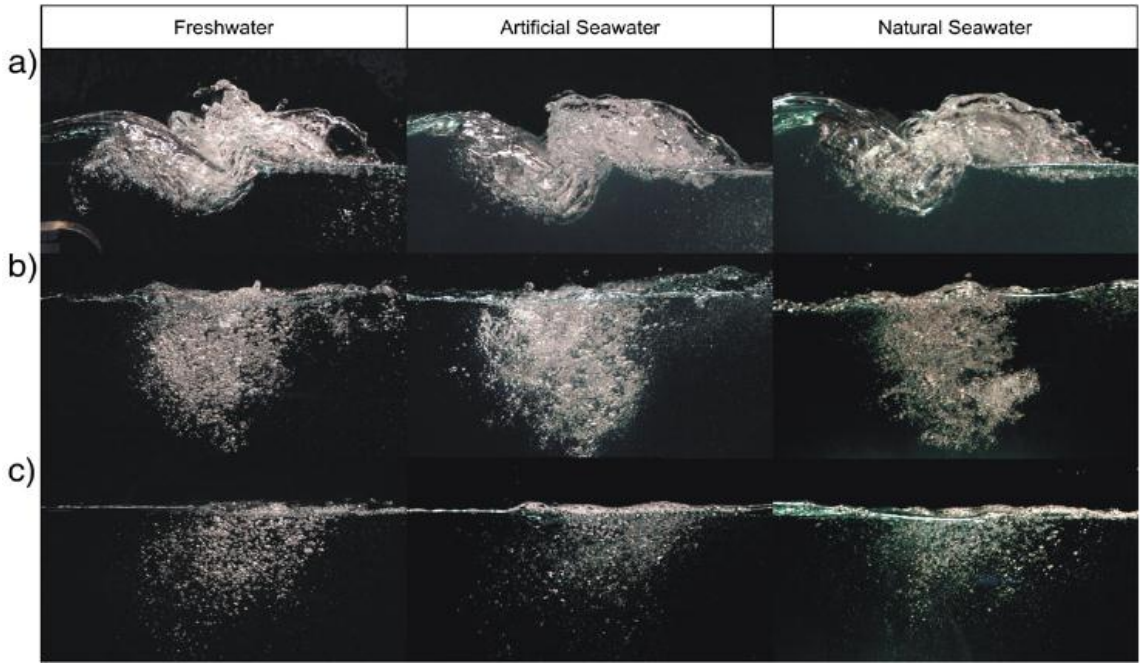

Figure 2.18: Photographs of the bubble plume evolution from the tenth wave in the series. (Blenkinsopp and Chaplin, 2011)

Since it is highly impractical to use seawater in a laboratory experiment, any research related to coastal and ocean engineering will utilize freshwater as the medium and the results are likely to be subjected to scale effects due to properties differences.

2.5.2 SURFACE TENSION

Surface tension is the intermolecular forces of the surface of a liquid that resists an external force. Tirindelli et al. (2000) reported that the surface tension of water increases when the steepness of waves increases due to a decrease in the mean curvature radius of the waves. Surface tension and viscosity have strong inter-related effects particularly near the sharp crest of a breaking wave where the mean radius is small.

The type of water (i.e. seawater and freshwater) has some influence on the surface tension of the liquid domain. Seawater has weaker surface tension than freshwater, and the weak tension has a fragile hold on the coalescence of water. When seawater waves rises up to maximum height, the crest of waves tend to form into plunging jets that collapses and generate large amount of bubbles. On contrary, freshwater that has stronger surface tension will not break the cohesion of the surface easily. Instead of forming a jet, the surface tension force will withstand the pull and form a bulge instead. As a result, the wave breaking of freshwater generates a lower volume of bubbles as compared to the seawater. The process of wave breaking involving weak and strong surface tension can be seen from Figure 2.19.

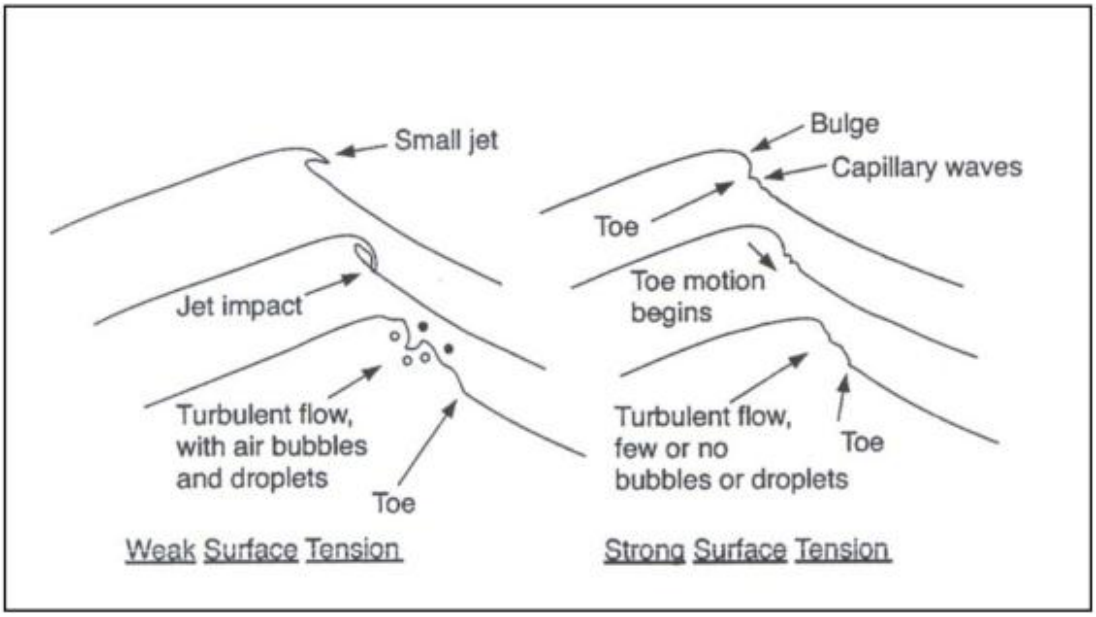

Figure 2.19: Schematic showing three phases of spilling breaking for weak and strong surface tension effects. (Tirindelli et al., 2000)

Hughes (1993) stated that scale effects due to surface tension will only be considered as significant when wave periods are shorter than 0.35 seconds and water depth is below 2cm. When these requirements are met, surface tension will then be considered as a dominant force and Weber law will be applied. Froude scaling will be considered invalid as Froude number does not represent the effects of surface tension and viscosity.

2.5.3 AIR CONTENT

Generally, air in a breaker curl exists in three states, i.e. expelled, entrapped and entrained. By definition, air is considered as 'expelled' if it remains connected to a body above the water (Tirindelli et al., 2000). If the air is expelled normally, and no significant mixture of air and water takes place, then the pressure will rise slowly as in accordance with the Froude numbers. The air that is separated and trapped by the plunging jet is known as entrapped air. The pressure of entrapped air may be quite different from the atmospheric pressure as they are often compressed or partially entrained by the breaking wave. Entrained air in the water column is usually a result of breakers, from either spilling or plunging in the form of bubbles, as shown in Figure 2.20.

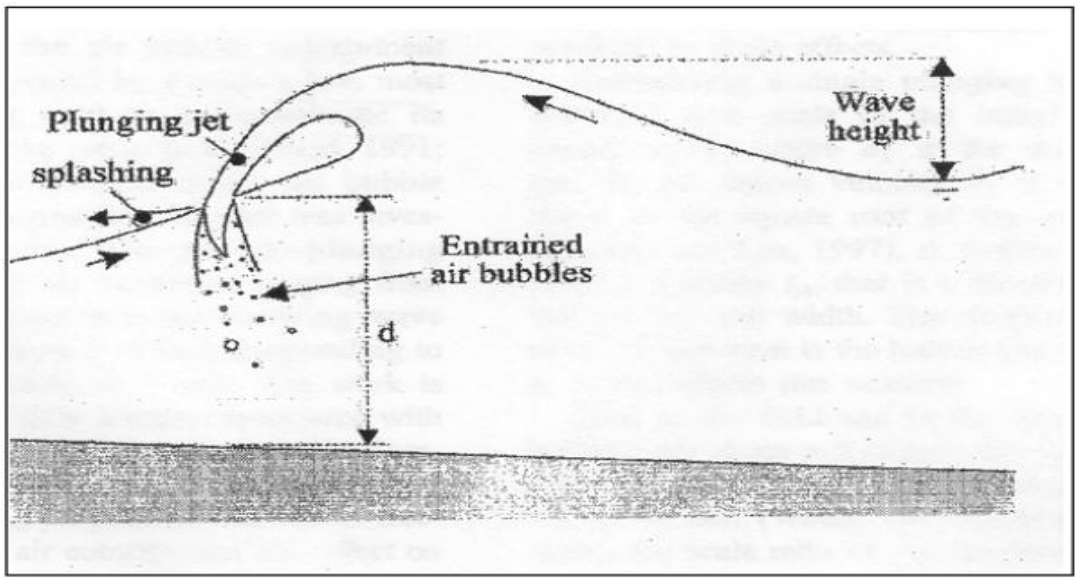

Figure 2.20: Plunging breaking wave (Tirindelli et al., 2000)

Andersen et al. (2011) reported that entrained air may escape from the water by rising to the surface as bubbles or by dissolving in the water. The varying

dimensions of the bubbles influence their rise velocity, capillary excess pressure, and dissolution rate. The greater the dimension of the bubbles, the higher the rising velocity and break off from the water body (Tirindelli et al., 2000).

The air entrainment process is highly dependant on various factors, most of them stemming from the fluid's characteristics such as the temperature, salt concentration, ionic structure, surface tension and viscosity. These factors will determine the number and size distribution of the bubbles. Slauenwhite and Johnson (1999) discovered that the formation of seawater bubbles are generally about 4-5 times more than freshwater, but smaller, as shown in Figure 2.21.

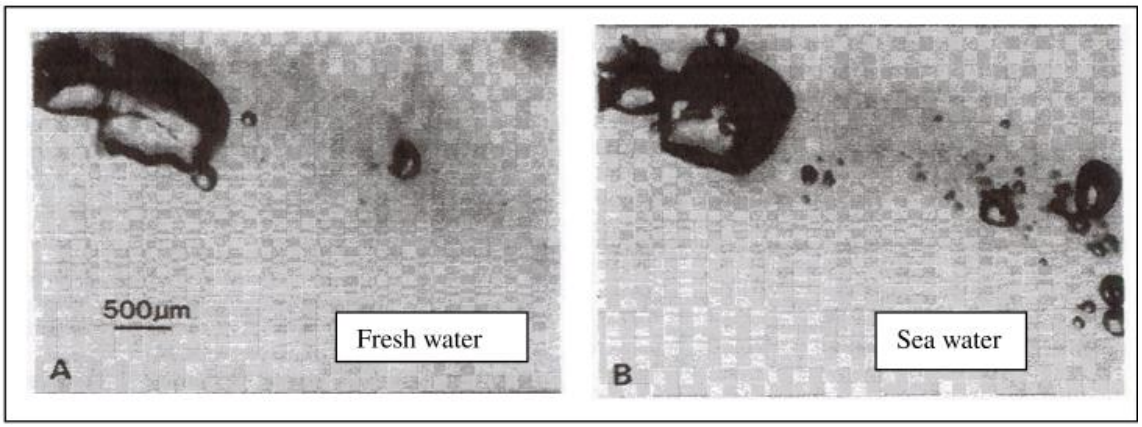

Figure 2.21: Examples of bubble sizes for entrained air in fresh and seawater (Tirindelli et al., 2000)

Craig et al. (1993) discovered that freshwater bubbles has a greater tendency to coalesce and escape from the water due to its high buoyancy, whereas the seawater's ionic structure tend to inhibit the movement of the bubbles. The bubbles in the seawater which are generally small will have a difficult time to escape from the water as it rises to the surface slowly. In fact, there will be a large scale difference between the model and the prototype, even though in the experiment it would seem that the generation of bubbles does not differ as much. This statement is supported by the fact that although the laboratory breakers in freshwater may disperse almost instantly by the next wave, the small bubbles of seawater will not disperse immediately, and will persist from one wave to the next (Blenkinsopp and Chaplin, 2011). In the full scale of prototype, a larger number of small bubbles will persevere and accumulate from one wave to another.

2.5.4 VISCOSITY AND FRICTION

Viscosity is a measure of fluid's resistance to relative motion within the fluid whereas the internal friction is the resistance of the fluid against the boundary walls. Hughes (1993) reported that models that are scaled geometrically according to Froude criterion does not stimulate viscous and frictional effects correctly as the Reynolds number depicting the flow are different between the prototype and model. Waves are also attenuated by internal friction and boundary layer friction arising from water viscosity. The difference in frictions between experimental boundary and sandy beaches may result in varying magnitude of wave decay between prototype and model. However this is usually considered as unimportant for short-wave models experimenting on short distance waves as the value of wave decay is usually insignificant over short distance.

Wave decay due to viscous friction can be calculated using Keulegan's (1950) formula:

$$\Omega = \frac{2}{BC}\sqrt{\frac{\pi V}{T}}\left[\frac{sinh\left(\frac{4\pi d}{L}\right)+\frac{2\pi B}{L}}{sinh\left(\frac{4\pi d}{L}\right)+\frac{4\pi d}{L}}\right] \tag{2.9}$$

$$\frac{H_2}{H_1} = e^{-\Omega x_p} \tag{2.10}$$

where,

Ω = friction factor

B = width of wave tank

C = wave celerity

V = kinematic viscosity

T = wave period

d = water depth

L = wavelength

H_1 = wave height at $x_p = 0$

H_2 = wave height after travelling distance x_p

p = density of water

Wave decay due to internal friction can be calculated using Keulegan's (1950) formula:

$$\psi = 8\pi^2 v \tag{2.11}$$

$$\frac{H_t}{H_i} = e^{-\psi t} \tag{2.12}$$

$$Distance = \frac{Lt}{T} \tag{2.13}$$

where,

ψ = friction factor

$\frac{H_t}{H_i}_t$ = wave decay ratio

L = wavelength

t = time

v = kinematic viscosity

T = wave period

2.6 SCALING LAWS FOR SCALE EFFECTS

There are various kinds of forces acting on water waves, namely inertia, gravity, viscous, elastic, and surface tension forces. To produce a model layout as similar to the prototype as possible, the relevant forces that are scalable should be scaled down accordingly.

2.6.1 FROUDE NUMBER

Froude Number is the ratio between inertia and gravity forces as shown below. It measures the relative importance of inertial forces acting on a fluid particle to the weight of the particle (Hughes, 1993). Data originating from physical models in which the central force is the wave action are usually converted to prototype scale by Froude law. Gravity and most fluid characteristics are almost equivalent in both model and prototype, therefore if the contrary is not specifically mentioned; it can be assumed that they are being maintained.

$$Fr = \frac{U}{\sqrt{gl}} \quad (2.14)$$

where,

Fr is Froude number,

U is velocity,

g is gravitational acceleration, and

L is length.

For any variable *X*, let n_x be the ratio among corresponding variables in prototype and model: $n_x = X_p/X_m$. Maintaining Froude number in model and prototype ($n_{Fr} = 1$), the following expressions for time (*t),* velocity (*U*) and pressure (*p*) scales can be derived.

$$n_t = n_U = n_l^{1/2} \quad (2.15)$$

$$n_p = n_l \quad (2.16)$$

Froude similarity ($F_m = F_p$) is regularly applied in hydraulics, and it is most suited for models where friction effects are negligible since it will be considered as a statistically correct scaled modeling.

2.6.2 REYNOLDS NUMBER

Reynolds number is the ratio between inertial forces and viscosity of a particle. The typical Reynolds Number (Re) is defined as

$$Re = \frac{Ul}{v} \quad (2.17)$$

where,

Re is Reynolds number,

U is velocity,

l is length, and

v is kinematic viscosity.

Reynolds number varies in time and space under the action of waves. To maintain Reynolds number, the following expressions for scaling time, velocity and pressure scales can be derived:

$$n_t = n_l^2 \tag{2.18}$$

$$n_U = n_l^{-1} \tag{2.19}$$

$$n_p = n_l^{-2} \tag{2.20}$$

Reynolds number is used to determine the state of the flow in accordance to the following standards:

Re < 2300 : Laminar Flow

2300 < Re < 4000 : Transient Flow

Re > 4000 : Turbulent Flow

Generally, laminar flow is known to have high viscosity whereas turbulent flow has low viscosity. Hence it is very likely that breakwater models that are tested against turbulent flow will be subjected to insignificant scale effects due to viscosity friction. In the case that the viscosity becomes the predominant force, Reynolds scaling law has to be applied.

2.6.3 WEBER NUMBER

Weber number is the ratio among inertia and surface tension forces.

$$We = \frac{\rho U^2 l}{\sigma} \tag{2.21}$$

where,

We = Weber number l = length

U = velocity σ = surface tension

ρ = fluid density

It is important that this scaling law is used when air entrainment or surface tensions are relevant processes in the physical system. In these cases the ratio should be preserved leading to Weber scaling law. The following expressions for time, velocity and pressure scales can be derived:

$$n_t = n_\sigma^{-1/2} \cdot n_l^{3/2} \tag{2.22}$$

$$n_U = n_\sigma^{1/2} \cdot n_l^{-1/2} \tag{2.23}$$

$$n_p = n_\sigma \cdot n_l^{-1} \tag{2.24}$$

Weber number is used when the surface tension is considered as the predominant force.

2.6.4 CAUCHY NUMBER

Cauchy number is the ratio between inertia and elastic forces and is relevant for fluid-structure interactions. The typical Cauchy number is defined as:

$$Ca = \frac{\rho U^2}{E} \tag{2.25}$$

$$E \equiv dp/(\frac{d\rho}{\rho}) = 1/K, \tag{2.26}$$

where,

Ca = Cauchy number

E = modulus of elasticity

U = velocity

K = bulk modulus

ρ = fluid density

v = kinematic viscosity

g = gravitational acceleration

σ = surface tension

Cauchy number is related to Mach number that is the ratio among particle velocity and sound celerity. The formula of Mach number is shown below:

$$Ma = \frac{U}{c} = \frac{U}{\sqrt{E/\rho}} \tag{2.27}$$

The presence of a mixture of air and water, even when the quantity of air is extremely reduced, causes the compressibility of the liquid to heighten considerably. When pressure variation is very high, changes in air density may be important. In such cases, pressure density relationship becomes non linear and a single compressibility coefficient does not apply to the full compression process. When the compressibility is the dominant factor, conversion to prototype should be made by using Cauchy law. The elasticity of air-water mixtures depends on air content, which may be significantly different in prototype and model, and on ambient pressure, that does not scale as a small pressure perturbation and therefore, the effect of elasticity scale is expressly represented.

Maintaining Cauchy or Mach number, the following expressions for scaling time, velocity and pressure can be derived:

$$n_t = n_E^{-1/2} \cdot n_l \tag{2.28}$$

$$n_U = n_E^{1/2} \tag{2.29}$$

$$n_p = E \tag{2.30}$$

Since Cauchy number is used only when the inertial forces are large enough to cause changes in fluid compressibility, it has little application in coastal and ocean engineering as fluid is generally regarded as incompressible.

2.6.5 SELECTED SCALING LAW

The ratio between inertia and gravity forces (expressed by Froude number) is vital in wave hydraulic models to guarantee proper scale reproduction of waves. The effect of viscous damping in conventional reproduction of non-breaking laboratory waves is negligible if the water depths are greater than 2-3 cm and wave propagation is over a short distance. Surface tension may cause some scale effects on non-breaking laboratory wave propagation which are small and steep with heights and periods approximately below 2cm and 0.35s, respectively. Air entrapment may also be caused by surface tension during breaking waves. Compressibility of air-water

mixture is much different in prototype or model conditions, hence causing scale effects.

In general, none of the above scaling laws are able to provide accurate scaling for all processes in wave-related breakwater models. Main scale effects from prototype to model are due to:

i) Inherent properties of the fluid that does not scale appropriately, such as the viscosity, surface tension and air content,
ii) Interaction with compliant structures, and
iii) Qualitative differences in processes in field and laboratory like the obstruction of pores by algae and mussels in sea-water, reduced coalescence of air bubbles in sea-water.

Froude scaling law is believed to provide the closest similitude between the model and prototype as compared to other scaling laws. Cauchy law is unsuitable for coastal experiments as the fluid is considered incompressible, whereas Weber and Reynolds laws are used only when the surface tension and viscosity forces are considered as the predominant force.

CHAPTER 3

METHODOLOGY

This chapter discusses the development of H-type floating breakwater model and its geometrical properties which are thoroughly presented through detailed drawings. The introduction to test facilities and the measuring equipments used for the experiment as well as experimental set-up will be delivered in this chapter.

3.1 DEVELOPMENT OF H-TYPE FLOATING BREAKWATER

This study is a continuation from the previous studies of floating breakwater development. No changes or improvements were made to the model since the focus of this study lies on the performance of H-type floating breakwater with adjusted drafts in a wider range of parameters rather than the innovation of breakwater shape. The model for this study was fabricated with a scale of 1:10. Figure 3.1 shows the comparison in size between the previously studied models as well as the prototype.

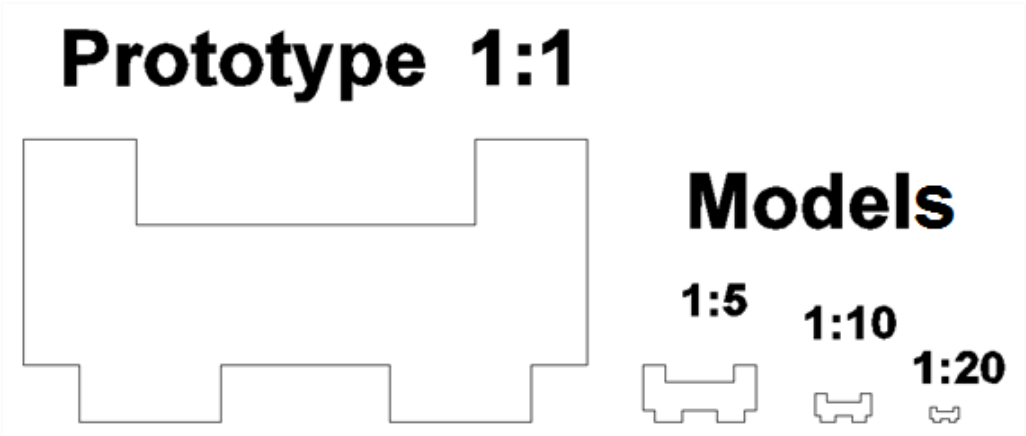

Figure 3.1: Size comparison between models and prototype

The model was constructed using plywood material that is coated with fiberglass. Plywood which is naturally lightweight keeps the model afloat while the fiberglass coating acts as a waterproof membrane to prevent water from seeping into the model. The model was installed with a 2 X 9 matrix compartments for weights placement. The compartment was covered by a transparent lid to prevent the intrusion of water. The weights placed in the compartments act as a mean to control the weight of the model which in turn affects the draft of the breakwater.

Figure 3.2 shows the isometric view of the model. The breakwater has a pair of upward arms and downward legs, both of which are attached to the box-shaped breakwater body. The seaward side of the breakwater acts as frontal barrier by reflecting most of the energy from incident wave. Some of the wave energy was lost in the vortex and turbulence of wave at the edge of the breakwater. When the incoming waves are higher than the upward arm of breakwater, the waves will overtop the model and get trapped between the two arms. The overtopping wave will then lose the momentum from shear stress or frictional loss.

The legs of the breakwater act as the secondary barrier against incoming waves by obstructing the wave motion beneath the breakwater. Waves that do get past the protective mechanisms of breakwater are termed as transmitted waves. The sides of the breakwater facing the flume walls were covered with polystyrene foam board to reduce the movement of the breakwater against the walls. Four hooks were attached to the bottom of the model for mooring purposes. A taut leg configuration was adopted in the experiments as it provides greater efficiency to the performance of floating breakwaters. A thin metal cable with low elasticity was tied to each hook while the other end was attached to the floor of wave flume. The lines were almost straight with minimal slacking. The pre-tensile force of mooring cables is zero in still water level and Figure 3.3 shows the typical cross-section of the model and the dimensions of the breakwater model are shown in Figure 3.4. Figure 3.5 and Figure 3.6 demonstrate the side view of outer and inner body of the model. The plan view of the model can be seen in Figure 3.7 and its cross-section is shown in Figure 3.8. Figures 3.9 and 3.10 shows the prepared model prior and after it was placed inside the wave flume.

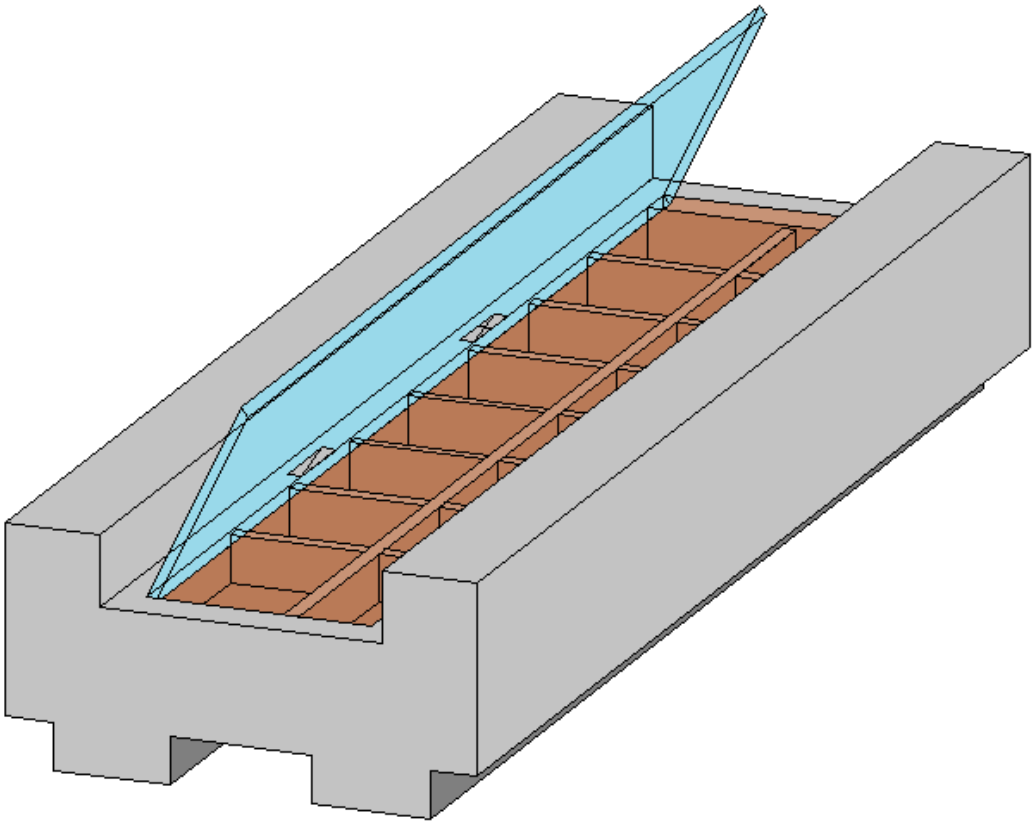

Figure 3.2: Isometric view of model

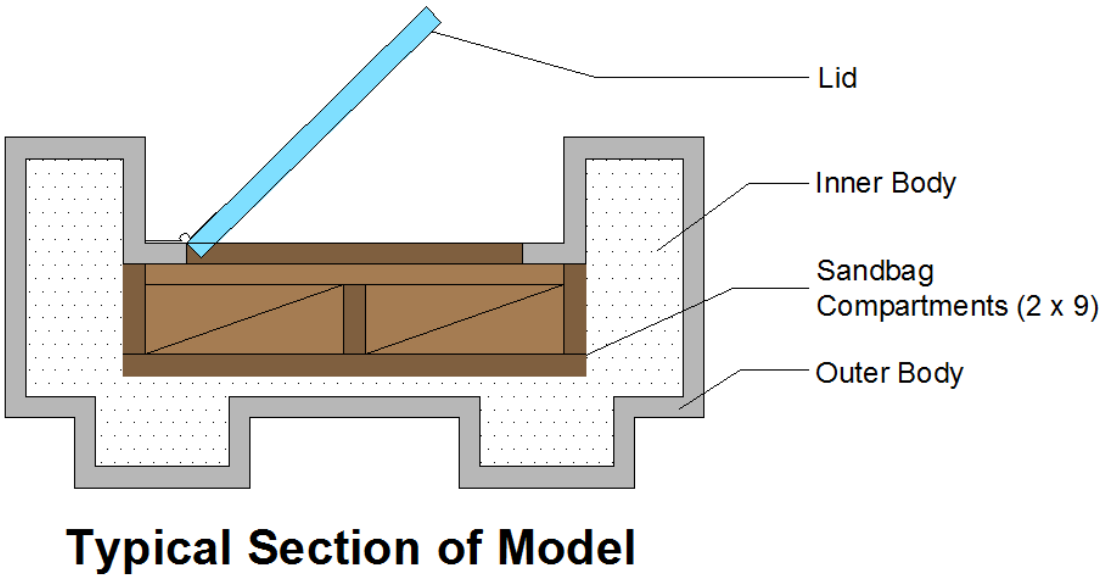

Figure 3.3: Typical section of model

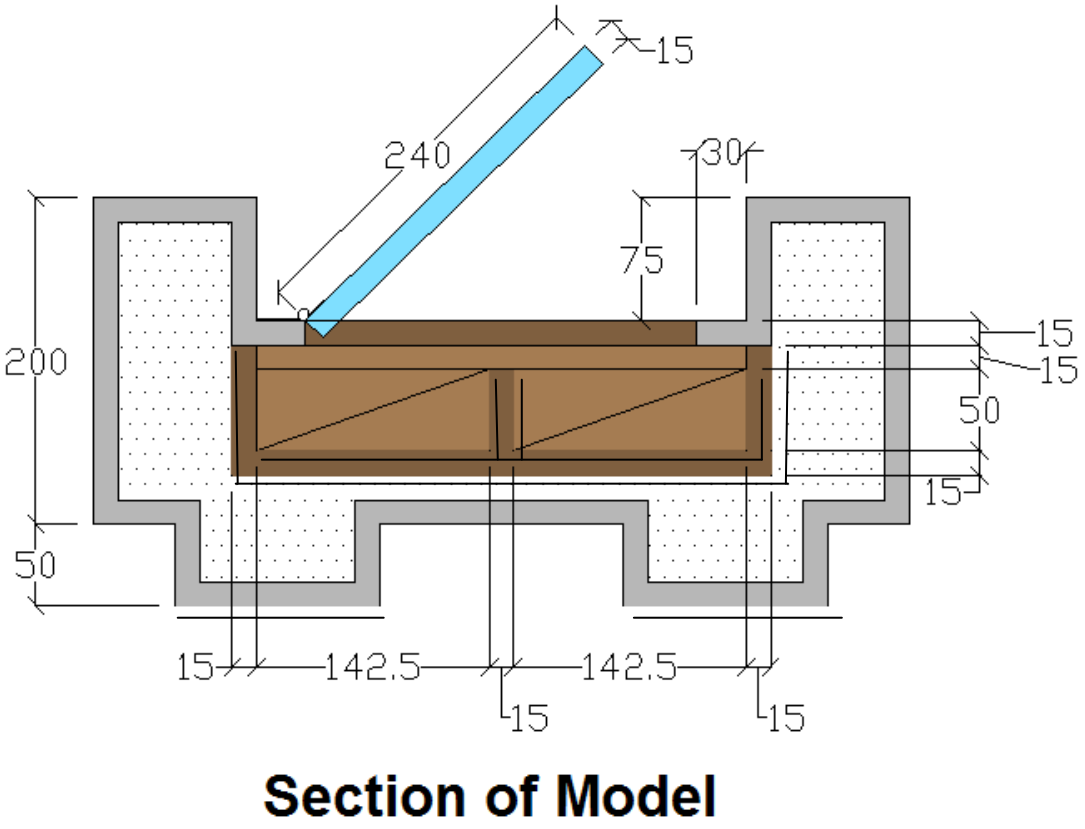

Figure 3.4: Dimensions of H-type floating breakwater model

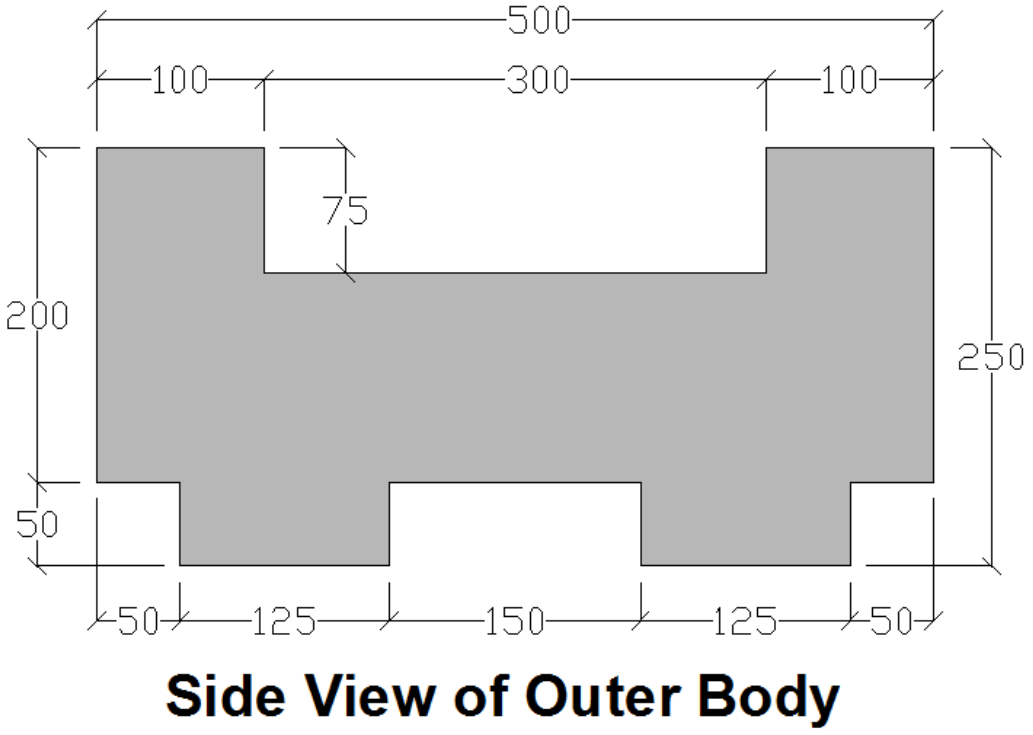

Figure 3.5: Side view of outer body

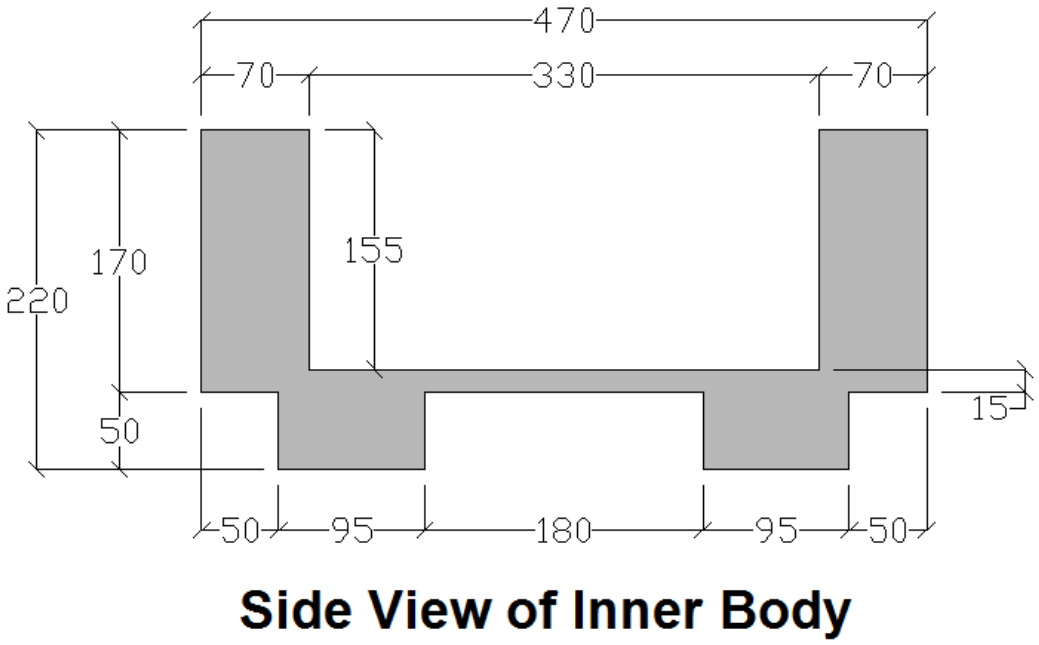

Figure 3.6: Side view of inner body

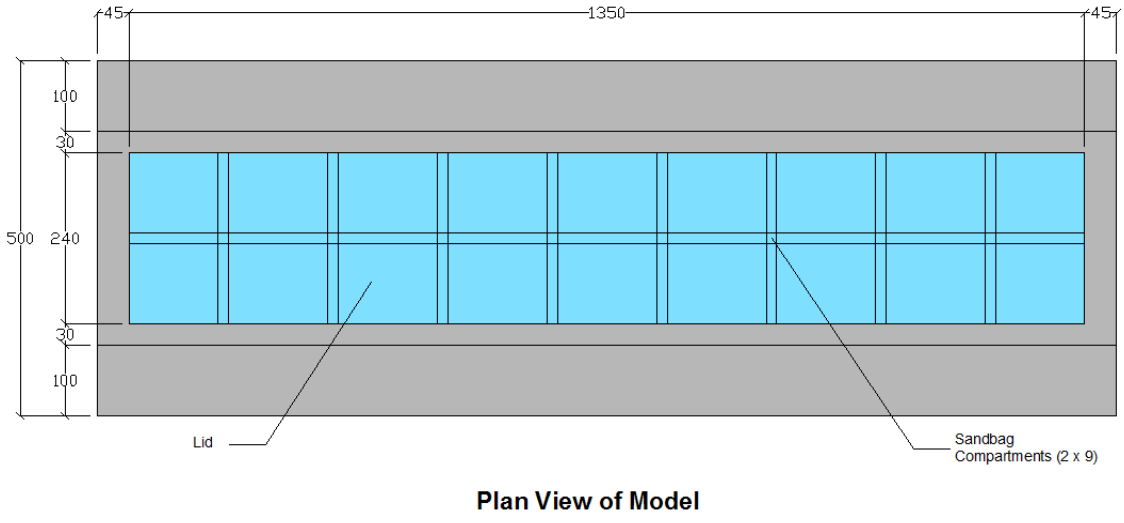

Figure 3.7: Plan view of model

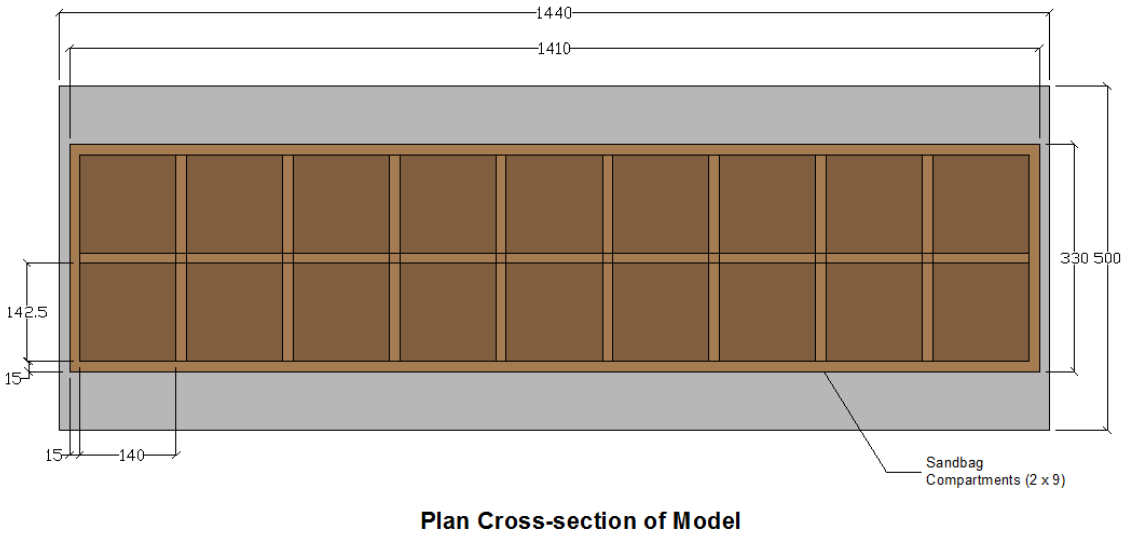

Figure 3.8: Plan cross-section of breakwater model

Figure 3.9: Preparation of model

Figure 3.10: Positioning of model

3.2 TEST FACILITIES AND EQUIPMENTS

The study was conducted in Offshore Laboratory (Block A) at Universiti Teknologi Petronas (UTP). The main facilities provided in the Offshore Laboratory of UTP are wave tank and wave flume, with the latter part being the key facility for this study. Other equipments and devices that were used in this study are provided in the laboratory as well.

3.2.1 WAVE FLUME

The experiments took place in a 25m long, 1.5m wide and 1.5m high wave flume as shown in Figure 3.11. The maximum water level permitted by the flume is 0.7m with a maximum allowable wave height of 0.2m. The walls of the wave flume were constructed using reinforced concrete. There are six panels of Plexiglass that were embedded along the flume with 3 on each side. The glass panels are placed to ease the observation and monitoring on the experiments that are being conducted inside the wave flume.

Figure 3.11: Wave flume

3.2.2 WAVE PADDLE

The wave paddle in Figure 3.12 is responsible for generating waves according to specifications for testing and experimenting purpose. It is installed at one end of the wave flume and is powered by an electric motor. This wave paddle, which was fabricated by Edinburgh Design Ltd, UK, is a piston-type wave generator (pneumatic-type) that can generate both regular and irregular waves. The maximum hinge depth of the wave paddle is 0.72m with a width of 1.2m. The paddle can produce wave height up to 0.3m and wave period up to 2 seconds. The wave paddle is made of anti-corrosive materials and is able to absorb reflected waves.

Figure 3.12: Wave paddle

3.2.3 WAVE ABSORBER

Wave absorber is a device placed at the other end of the wave flume with the purpose of minimizing the reflected waves in the wave flume. This device is important to avoid any errors to the readings of reflected and transmitted wave heights due to remaining wave energy of the previous waves. Figure 3.13 shows the wave absorber that is about 3m in length and is made of anti-corrosion material with the ability to absorb 90% of wave energy.

Figure 3.13: Wave absorber

3.2.4 WAVE PROBES

Wave probes were used to measure the incident wave height, reflected wave height and transmitted wave height in the flume. They were placed on both sides of the model; three probes on each side. This is in accordance to the 3-point method (Mansard and Funke, 1980). Figure 3.14 shows the probes being arranged in a straight line perpendicular to the model and the wave paddle. The maximum measurement of wave height is 0.4m and 128Hz for wave frequency. Calibration of probes was done prior to conducting any tests to avoid any measurement errors.

The probes facing the wave paddle were used to measure the incident and reflected wave heights, while the probes at the lee side of the model were meant to measure the transmitted wave height and the reflected waves from the wave absorber (if any). Data obtained from the wave probes were used for calculation to separate the incident and reflected wave spectra from the co-existing wave spectra by using the 3-points method developed by Mansard and Funke (1980). This method is based on least square analysis and is far superior to the 2^{nd} point method in regards of frequency range, sensitivity to noise and lesser deviation or distraction from the linear theory.

Figure 3.14: Wave probes

3.2.5 DATA LOGGER/ACQUISITION SYSTEM

The wave paddle and wave probes that were set up in the wave flume are connected to the computer. The characteristics of generated waves can be specified through the computer to set up the required testing and experimental condition. The computer then sends the command to the wave paddle through the connection. The wave probes were also fixed to a data logger that records the measurement of wave heights and transfers the data to the computer for further analysis.

3.3 EXPERIMENTAL SET-UP

Figure 3.15 and Figure 3.16 illustrates the experimental set-up of the study. The model placed between the probes was moored to the mid-section of the flume about 13m away from the wave paddle. The model was anchored to the floor using anchors and hooks which were connected to the bracing of the model. Three wave probes were placed on each side of the model in accordance to Mansard and Funke's (1980) 3-points method. Another wave probe was placed 1m away from the model at both seaward and leeward side of model to capture the reflected and transmitted

wave heights by the model. Cameras were installed around the model to capture the movement and wave interactions of the model. The position of model was unchanged but the wave probes spacing were adjusted according to the test conditions.

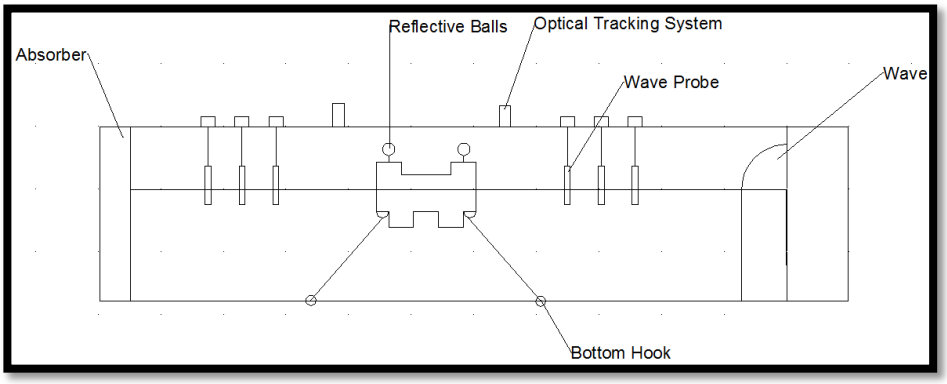

Figure 3.15: Experimental set-up – side view (not subjected to scale)

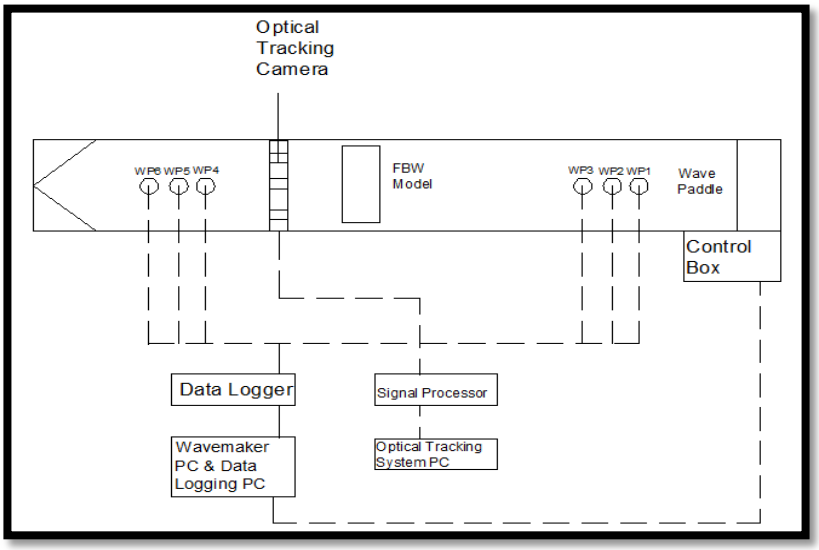

Figure 3.16: Experimental layout (not subjected to scale)

The time series of data were analyzed further to yield significant wave parameters i.e. significant wave height and peak wave period whereas the Mansard and Funke's method was adopted to decompose the wave signals from three probes into incident and reflected wave components.

3.4 TEST PROGRAM

The model was tested against several testing conditions similar to the previous studies. There were three manipulated variables that determined the test environment, i.e. the water draft (D), the wave steepness (H/L) and the wave period (T). Each of these components has its own range of testing values that were similar to the previous studies in which the model was subjected to. The variation of these variables can be seen in Table 3.1. Upon altering the variables, the spacing of the wave probes needs to be adjusted accordingly. The model was tested against irregular waves to simulate realistic sea condition.

Table 3.1: Values of Dependant Variables

Dependant Variables	Values
Wave Steepness, H/L	0.04
	0.06
	0.08
Wave Period, T (sec)	0.8
	1.0
	1.2
	1.4
Breakwater Draft, D/d (m)	0.1143
	0.1714
	0.2286

Total test runs = 3 wave steepness X 4 wave periods X 3 breakwater drafts
= 36 tests

The 3 wave steepness corresponds to 3 different wave heights for each wave period, whereas the breakwater draft was changed using the weights for every set of completed wave periods and wave heights.

3.5 PRELIMINARY CALCULATION AND ANALYSIS

Preliminary study and calculations were done to give an insight into possible results in regards to scale effects on physical modeling. The factors affecting scale effects were given consideration in this preliminary study.

3.5.1 PROPERTIES OF SEAWATER

Differing properties between seawater and freshwater will result in varying formation of bubbles. However the previous models were tested in similar condition with freshwater as the liquid medium. There are no varying properties of liquid between the experimental settings of the models. Therefore no scale effects due to properties difference may be detected between the experimental results. The results however may be subjected to scale effects if it is used for prototype. It is assumed that the properties of seawater will not play a major role in causing significant scale effect on the study.

3.5.2 SURFACE TENSION

Hughes (1993) mentioned that significant scale effects due to surface tension can only occur when the wave periods are shorter than 0.35s and the water depth is below 2cm. Since the water depth for the experiment will be fixed at 0.7m and the wave periods selected ranges from 0.7s to 2.0s, it can be safely deduced that surface tension will not cause any major or significant scale effects on the model.

3.5.3 AIR CONTENT

The amount of air content that will persist in the water may differ according to the scale of model and testing environment. The amount of bubbles entrained in the water will be larger and persists longer with increasing model scale (Blenkinsopp and Chaplin, 2011). It is anticipated that the varying amount of air content will cause considerable scale effects on the model.

3.5.4 VISCOSITY AND FRICTION

The process of wave breaking is often chaotic and greatly disrupts the wave formation. The flow of water around the breakwater is assumed as turbulent waves. Table 3.2 shows theoretical calculation on the Reynolds number of the subjected flow. Based on the table, the Reynolds numbers of the selected wave periods are well beyond 4000, in which the viscous scale effects may be considered as insignificant.

Table 3.2: Theoretical calculation of Reynolds number of the flow

Tp (s)	*U (m/s)*	ν	*Re*
0.7	3.571429	1.00E-06	1.78E+06
0.8	3.125	1.00E-06	1.56E+06
0.9	2.777778	1.00E-06	1.38E+06
1.0	2.5	1.00E-06	1.25E+06
1.1	2.272727	1.00E-06	1.13E+06
1.2	2.083333	1.00E-06	1.04E+06
1.3	1.923077	1.00E-06	9.58E+05
1.4	1.785714	1.00E-06	8.89E+05
1.5	1.666667	1.00E-06	8.30E+05
1.6	1.5625	1.00E-06	7.78E+05
1.7	1.470588	1.00E-06	7.32E+05
1.8	1.388889	1.00E-06	6.92E+05
1.9	1.315789	1.00E-06	6.55E+05
2.0	1.25	1.00E-06	6.23E+05

Possible wave decay may also occur due to the boundary friction resulted by the flume surfaces. Further investigation on wave decay due to internal viscous friction was done by using Keulegan's (1950) formula to check the level of wave decay. Table 3.3 and Table 3.4 show the percentages of wave decay for wave periods 0.7s to 2.0s at distances of 2.5m and 25m, respectively, from the wave paddle. From the calculation done, it can be concluded that the wave decays are only apparent over long distance travel and rather insignificant for short distances. For example, the 8s wave period will have a decay percentage of 0.5286% and 5.1622% for 2.5m and 25m, respectively. Since the breakwater model will be placed in an intermediate distance from the wave paddle, it is assumed that the value of wave

decay upon hitting the breakwater model is inconsequential. Overall, the viscosity and friction forces can be said to be negligible in regards of scale effects.

Water Temperature θ (°)	20	Wave tank width B (m)	1.5
Density of Water ρ (kg/m^3)	999.63	Initial wave height H_1 (m)	0.25
Dynamic Viscosity of water μ (kg/ms)	0.001002	Water depth (m)	0.7
Kinematic viscosity ν (m^2/s)	1.004		

Table 3.3: Percentage of wave decay due to internal viscous friction for distance of 2.5m

Tp (s)	*L (m)*	*C (m/s)*	*4πd/L*	ϕ_1	ϕ_2	Ω	H_2	*%*
0.7	0.765	1.093	11.49863978	49303.11	49302.29	0.00259	0.248387	0.6453
0.8	0.999	1.249	8.805264695	3344.066	3343.437	0.00212	0.248678	0.5286
0.9	1.262	1.402	6.970253114	539.7137	539.2159	0.001782	0.248889	0.4445
1.0	1.551	1.551	5.671476099	151.3063	150.9012	0.001531	0.249045	0.3820
1.1	1.856	1.687	4.739471676	62.26051	61.92198	0.001346	0.24916	0.3359
1.2	2.171	1.809	4.051800751	33.08297	32.79356	0.001206	0.249248	0.3009
1.3	2.489	1.915	3.534133961	20.90464	20.65221	0.001098	0.249315	0.2741
1.4	2.805	2.004	3.135992667	14.84400	14.62000	0.001014	0.249367	0.2532
1.5	3.118	2.079	2.821186475	11.39132	11.18980	0.000947	0.249409	0.2364
1.6	3.427	2.142	2.566810455	9.223872	9.040529	0.000892	0.249443	0.2227
1.7	3.731	2.195	2.357668033	7.761894	7.593489	0.000846	0.249472	0.2112
1.8	4.032	2.240	2.181661565	6.711576	6.555743	0.000807	0.249496	0.2015
1.9	4.329	2.278	2.031984160	5.926193	5.781051	0.000773	0.249517	0.1931
2.0	4.624	2.312	1.902348493	5.314429	5.178547	0.000743	0.249536	0.1856

Table 3.4: Percentage of wave decay due to internal viscous friction for distance of 25m

Tp (s)	*L (m)*	*C (m/s)*	*4πd/L*	ϕ_1	ϕ_2	Ω	H_2	*%*
0.7	0.765	1.093	11.49863978	49303.11	49302.29	0.00259	0.234328	6.2687
0.8	0.999	1.249	8.805264695	3344.066	3343.437	0.00212	0.237094	5.1622
0.9	1.262	1.402	6.970253114	539.7137	539.2159	0.001782	0.239107	4.3573
1.0	1.551	1.551	5.671476099	151.3063	150.9012	0.001531	0.240613	3.7548
1.1	1.856	1.687	4.739471676	62.26051	61.92198	0.001346	0.241729	3.3082
1.2	2.171	1.809	4.051800751	33.08297	32.79356	0.001206	0.242578	2.9688
1.3	2.489	1.915	3.534133961	20.90464	20.65221	0.001098	0.243232	2.7071
1.4	2.805	2.004	3.135992667	14.84400	14.62000	0.001014	0.243742	2.5030
1.5	3.118	2.079	2.821186475	11.39132	11.18980	0.000947	0.244152	2.3391
1.6	3.427	2.142	2.566810455	9.223872	9.040529	0.000892	0.244489	2.2046
1.7	3.731	2.195	2.357668033	7.761894	7.593489	0.000846	0.244769	2.0922
1.8	4.032	2.240	2.181661565	6.711576	6.555743	0.000807	0.245009	1.9965
1.9	4.329	2.278	2.031984160	5.926193	5.781051	0.000773	0.245215	1.9141
2.0	4.624	2.312	1.902348493	5.314429	5.178547	0.000743	0.245398	1.8409

3.5.5 SELECTION OF SCALING LAW IN PHYSICAL MODELING

The most suitable scaling law for scale effects study is the Froude similitude which relates the inertia and gravity forces. This law is chosen assuming that the effects of surface tension and viscosity forces are negligible. With that assumption, both Weber and Reynolds numbers are considered unsuitable for this study as these scaling laws are centered on surface tension and viscosity forces, respectively. Cauchy scaling law is also considered unsuitable for coastal engineering studies as fluids are considered incompressible. Models that are scaled in accordance to the Froude criterion are scaled geometrically with the assumption that all other forces are insignificant.

3.5.6 SUMMARY OF PRELIMINARY STUDY

From the preliminary theoretical analysis, the scale effects on wave interactions of H-type floating breakwater are considered insignificant. This indicates that the data obtained from the experiments are readily usable for the prototype. However it is important to note that these assumptions were made merely based on the desk study. A specific experimental study on scale effects may validate the proposed hypothesis of scale effects associated with physical modeling.

3.6 ANALYSIS OF DATA

The results obtained were analyzed by first plotting the elevation of water depth from each probe against time which would comprise of both incident and reflected wave heights. The set of data signals were then decomposed into incident and reflected spectra using Fast Fourier Transform method. All of the analyses were done by applying functions and formulae using MATLAB program.

CHAPTER 4

RESULTS AND DISCUSSION

This chapter delivers brief explanation on wave flume and wave probe calibrations as well as the prerequisite of experimental study such as gain value and script programming. The calculated experimental values for specific wave generation and wave probe spacing are included followed by the experimental results on the performance of H-type floating breakwater and its analysis.

4.1 WAVE FLUME & WAVE PROBE CALIBRATIONS

The calibration of wave flume is simply the checkup on the working condition of the flume as a whole, including the water pumping ability and the operating of equipments and devices required for this study.

Wave probes on the other hand, were calibrated in accordance to Mansard and Funke‘s (1980) 3-point method, as being mentioned in the previous chapter. The basis of this method is to measure simultaneously the waves in the flume at three different points with adequate distances between one set of probe to another. The wave probes were placed in a straight line perpendicularly to the wave paddle inside the wave flume. The set up of all the equipments for the calibration is shown in the Figure 4.1, where it indicates the length of the probes from the wave paddle (*X1*), the length of first probe to the second probe ($X1 = L_p/102$) and the length of first probe to the third probe ($L_p/6 < X13 < L_p/3$).

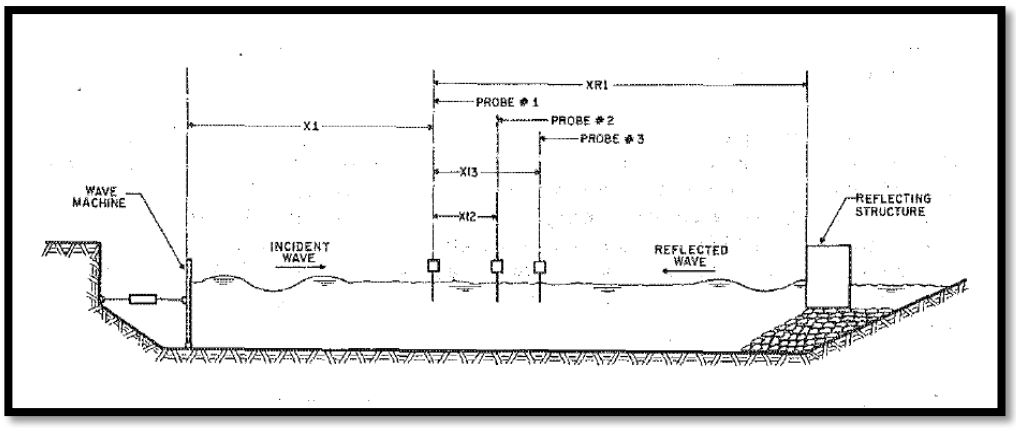

Figure 4.1: Three-point method calibration set

Where L_p is the wavelength of that particular wave period. This spacing requirement is important to ensure that there are no singularities in the wave probe readings. The spacing of the wave probes corresponding to the wave period are shown in Table 4.1.

Table 4.1: Wave probe spacing

T (s)	L_p (m)	f (Hz)	Distance of probe 1 and 2 (cm)	Distance of probe 2 and 3 (cm)	Distance of probe 1 and 3 (cm)
0.8	1.00	1.250	10.0	15.0	25.0
1.0	1.55	1.000	15.5	28.0	43.5
1.2	2.17	0.833	21.7	28.0	49.7
1.4	2.81	0.714	28.1	40.0	68.1

The distance between the nearest wave probes to the reflective structures is defined as one wavelength or more. In this study, the distance was fixed at 3 meters since the maximum wavelength in this whole study is 2.81 meters.

4.2 RANDOM WAVES

This study was carried out against random waves to simulate realistic sea condition rather than simulating a controlled environment with regular wave condition. To program specific wave height in the wave generation software, a zero run was first carried out in an empty flume in a series of trial and error with various gain values to obtain the gain value graph for that specific water depth as shown in

Figure 4.2. This gain value graph is considered an important tool in generating specified wave height accurately and must be done prior to each study with varying water depth and experimental setting. It is not advisable to reuse gain value graphs that are more than few months old as the efficiency of the wave paddle may have decline since then and as a result, the aptitude may varies.

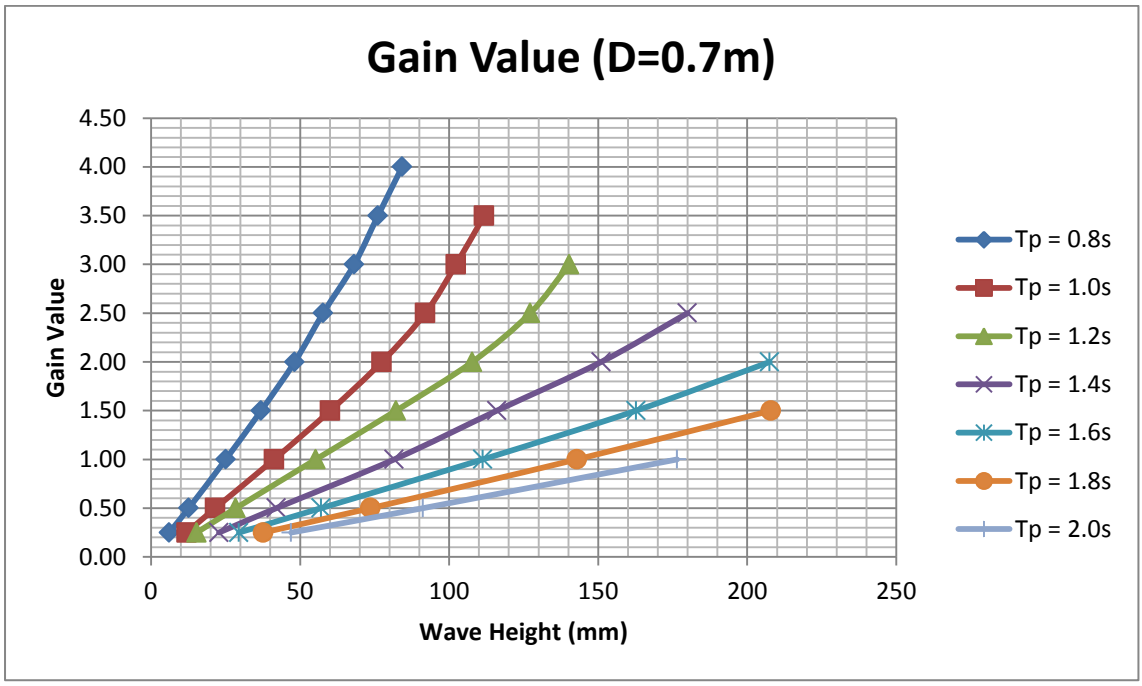

Figure 4.2: Gain Value for water depth of 0.7m

Based on this graph, the gain value needed to generate specific wave height of random waves can be determined and encoded into wave generation script. Table 4.2 shows the corresponding gain value for each wave height that was obtained from the gain value graph.

Table 4.2: Gain value for corresponding wave height and steepness

Wave Steepness, H/L		**0.04**		**0.05**		**0.06**	
Wave Period, T (s)	Wavelength, L (m)	Wave Height (m)	Gain Value	Wave Height (m)	Gain Value	Wave Height (m)	Gain Value
0.8	1.00	0.04	1.65	0.05	2.10	0.06	2.60
1.0	1.55	0.062	1.50	0.078	2.00	0.093	2.50
1.2	2.17	0.087	1.60	0.109	2.05	0.130	2.60
1.4	2.81	0.112	1.40	0.141	1.85	0169	2.30

Once the gain value had been obtained, it was incorporated into the following script to produce specific type of random waves. The following script is an example of coding for random wave generation:

“experiment "Calibration set" with ("UTP_700/default.ttf")

begin

run "1.0sec JONSWAP H/L=0.04 Hs=0.062 Gain=1.55" with (13)

wave x=1.55*jonswap(1.0,0.0081,3.3,0.07,0.09);

makewave x on 1;

end;

end; ”

In the command given, the wave paddle is expected to produce a JONSWAP wave of 0.062 meter tall with a peak frequency of 1Hz, or 1 second of wave period. The gain value used in this command to produce 0.062 meter tall waves in 1 second wave period is 1.55. The application of gain value will help in generating an accurate wave as specified for this experiment.

4.3 BREAKWATER DRAFTS

The effects of breakwater draft was studied by experimenting with three values of breakwater drafts which are basically the minimum draft, the maximum draft and the middle draft as shown in Figure 4.3 and summarized in Table 4.3.

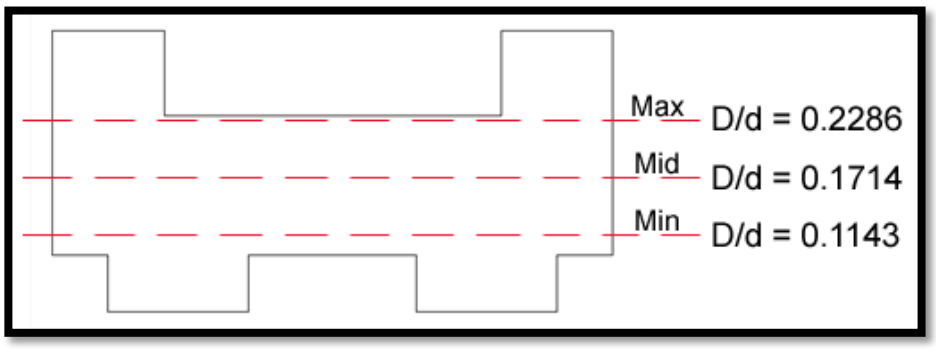

Figure 4.3: Breakwater drafts

Table 4.3: Submergence level of varying breakwater drafts

Level of breakwater draft	Depth of Submergence, D (m)	Water Depth, d (m)	Breakwater Draft, D/d
Maximum	0.16	0.7	0.2286
Middle	0.12	0.7	0.1714
Minimum	0.08	0.7	0.1143

4.4 EXPERIMENTAL RESULTS

Series of experiments were rigorously conducted in the wave flume to study the wave responses on the H-type floating breakwater in random waves. The details of the random wave types are presented in section 2.2. Some examples of raw data and the related wave analysis are demonstrated according to the wave type in this section.

Random waves are made up of a lot of regular plane waves with random wavelength, water level elevation and also wave phase. Figures 4.4 - 4.6 present the profiles of 1 second peak period waves with steepness H_i/L_p = 0.04, 0.05 and 0.06 of maximum breakwater draft of 0.2286 that were recorded by the wave probes at the closest proximity to the test model (i.e. WP4 and WP5) and the corresponding energy density spectra for incident, reflected and transmitted waves in random waves described by JONSWAP.

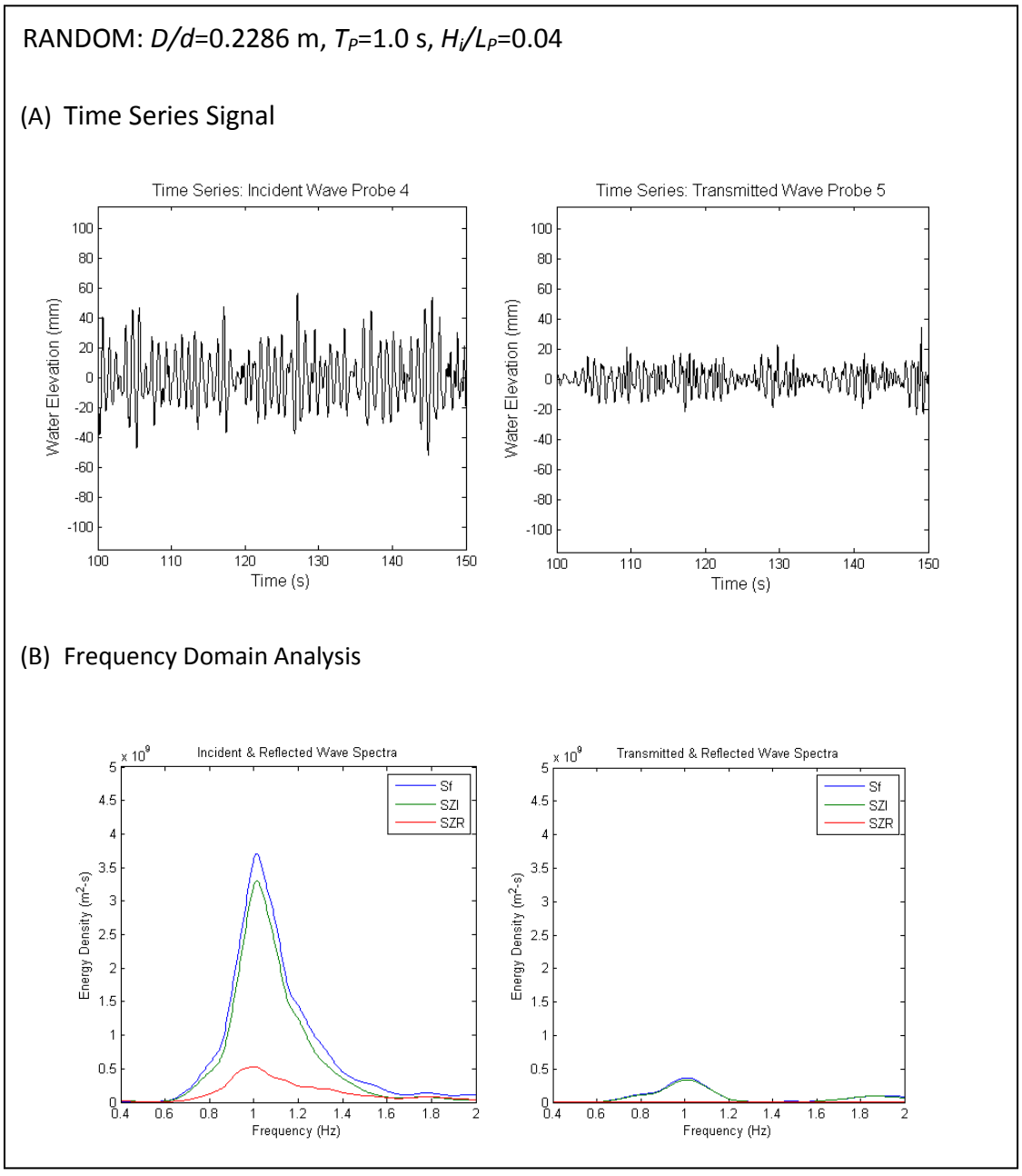

Figure 4.4: Time Series Signal and Frequency Domain Analysis for Random Waves (D/d=0.2286 m, T_P=1.0 s, H_i/L_P=0.04)

RANDOM: D/d=0.2286 m, T_P=1.0 s, H_i/L_P=0.05

(A) Time Series Signal

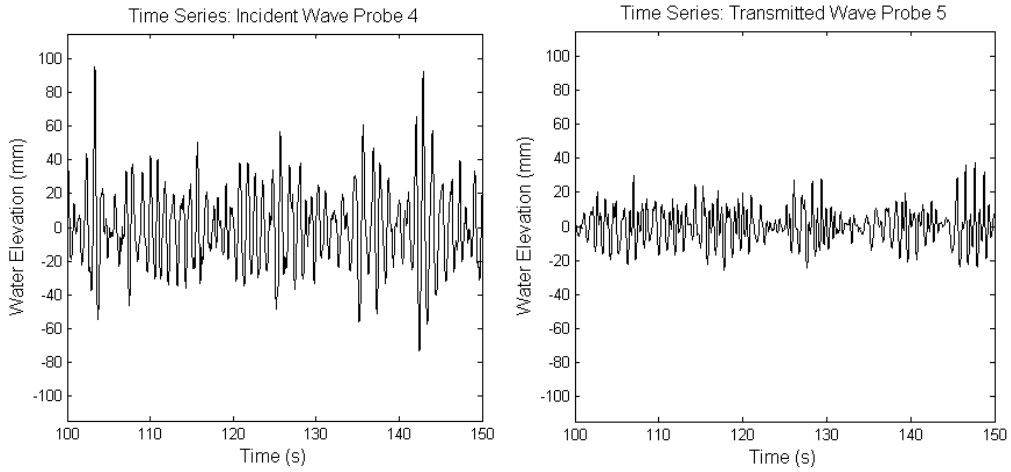

(B) Frequency Domain Analysis

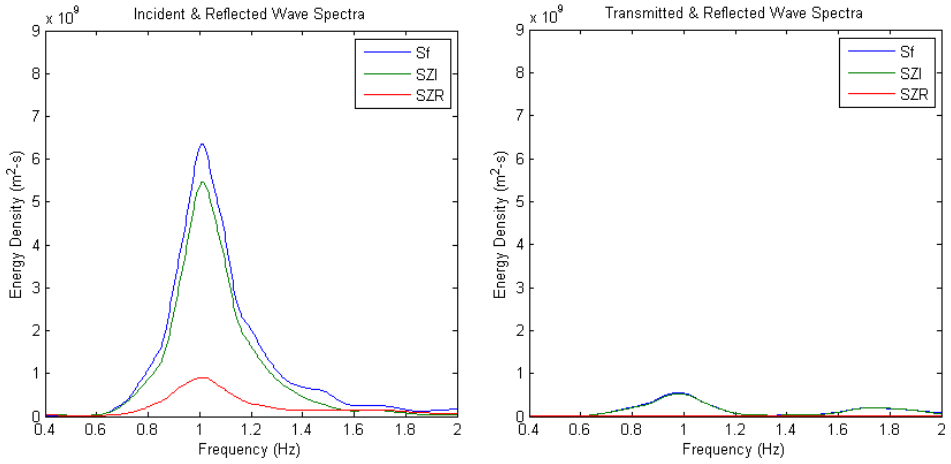

Figure 4.5: Time Series Signal and Frequency Domain Analysis for Random Waves (D/d=0.2286 m, T_P=1.0 s, H_i/L_P=0.05)

RANDOM: D/d=0.2286 m, T_P=1.0 s, H_i/L_P=0.06

(A) Time Series Signal

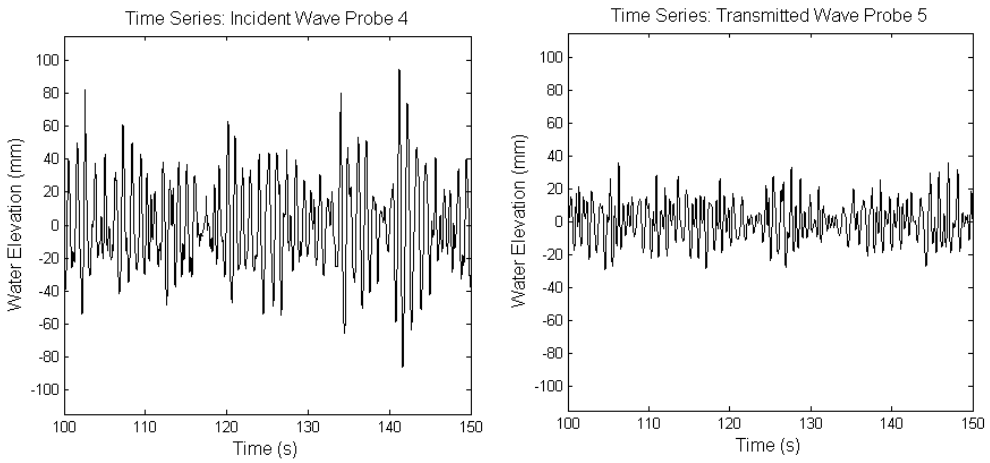

(B) Frequency Domain Analysis

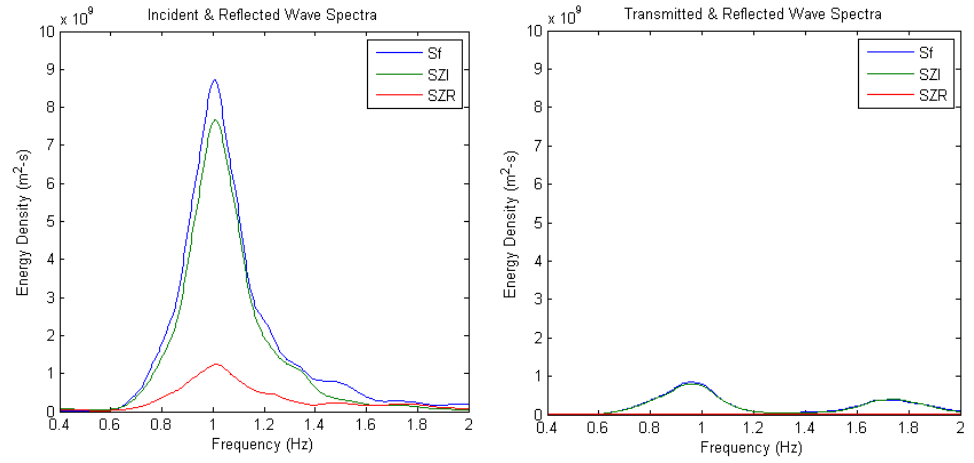

Figure 4.6: Time Series Signal and Frequency Domain Analysis for Random Waves (D/d=0.2286 m, T_P=1.0 s, H_i/L_P=0.06)

RANDOM: D/d=0.2286 m, T_P=1.4 s, H_i/L_P=0.04

(A) Time Series Signal

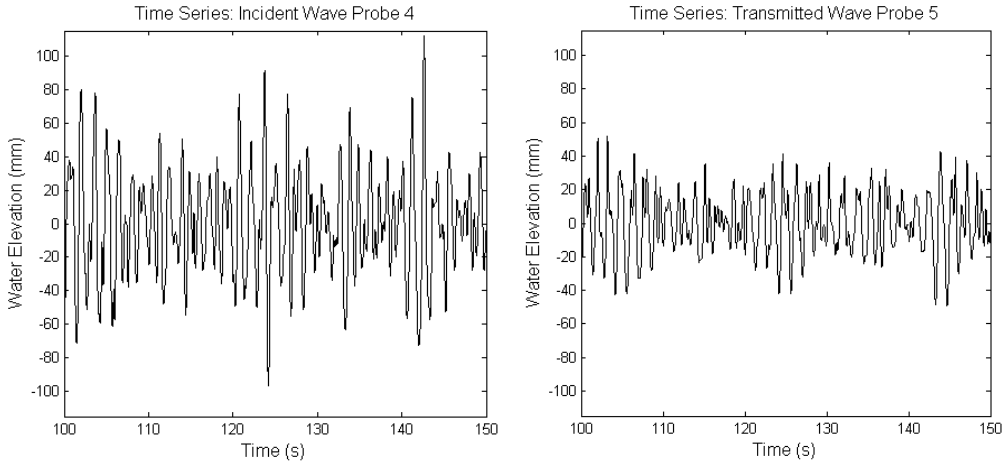

(B) Frequency Domain Analysis

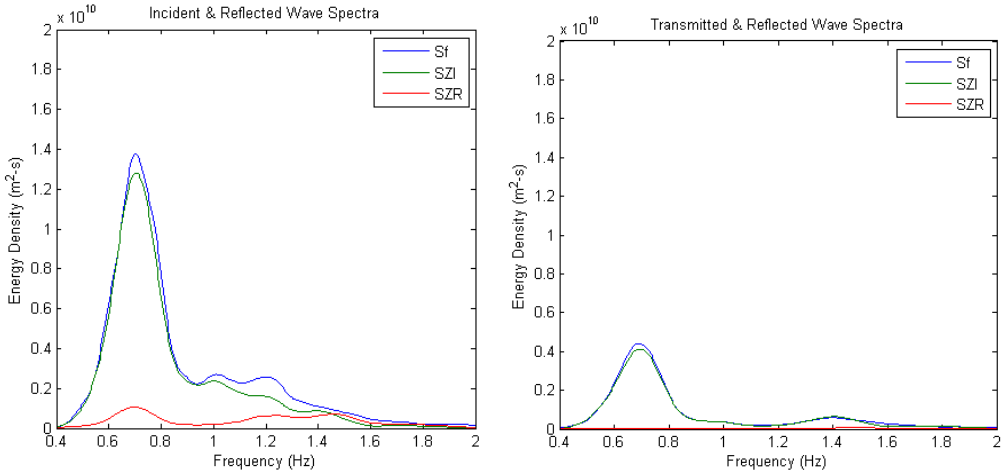

Figure 4.7: Time Series Signal and Frequency Domain Analysis for Random Waves (D/d=0.2286 m, T_P=1.4 s, H_i/L_P=0.04)

Figures 4.4 – 4.6 show the time series signal measured by wave probes 4 and 5 for H_i/L = 0.04, 0.05 and 0.06 are respectively plotted in a 50-s window with a start-up time of 100 s. The signal inputs for random waves are irregular with a range of wave periods and heights. The energy is unevenly distributed in a range of wave frequencies. The peak of the energy spectra indicates the peak frequency of the data set for incident, reflected and transmitted waves in random waves. Note that the area underneath the curves of energy spectra indicates the zeroth spectral moment m_0 whereby the energy is directly proportional to m_0. The findings obtained are similar to those of the regular waves in which the energy of the incident waves is considered the greatest, followed by the reflected and transmitted waves in all test cases; whereas, the reflected waves at the lee of the test model is negligible.

Figure 4.7 displays the time series and the related wave spectra analysis of a longer waves on the H-type floating breakwater subjected to breakwater draft, D/d=0.2286 , peak wave period T_p = 1.4 s and wave steepness H_i/L = 0.04. It is apparent from the plots that the incident waves carry more energy than the reflected waves from the test model. At the rear of the breakwater, the transmitted wave energy is considerably dampened by the test model due to abrupt reduction of the energy density level. It is also noted from the figures that the reflected wave energy behind the test model is so small that it can be ignored in the experiments. Analyses of other test series were also conducted; however, these outcomes of the analysis are not displayed here due to the page constraint of the thesis. It is worth mentioning that the trends of the results resemble those presented here.

4.5 RESULTS INTERPRETATION

4.5.1 EFFECT OF RELATIVE BREAKWATER WIDTH

The wave energy coefficients C_T, C_R and C_L are plotted against the breakwater width B/L where B and L are the breakwater width and the wavelength, respectively. The geometrical ratio of B/L is a well accepted dimensionless parameter used in the design of coastal engineering structures. Since B is fixed in this study and the fact that L is the only independent variable that is governed by the change of wave period or wave frequency, the B/L is often termed as the relative

wave period or the relative wave length. Nevertheless, as far as this thesis is concerned, the *B/L* is consistently termed as the relative breakwater width throughout this writing.

4.5.1.1 WAVE TRANSMISSION

Wave transmission performance of the H-type floating breakwater is quantified by the wave transmission coefficient, C_T. The lower the C_T values, the smaller the amount of wave transmission at the lee side of the breakwater which, in turn, leads to higher wave attenuation ability. Figure 4.8 displays the C_T of the H-type floating breakwater subjected to immersion depth ratios or breakwater drafts of *D/d* = 0.1143, 0.1714 and 0.2286 in random waves. The wave steepness tested ranges from 0.04 – 0.06.

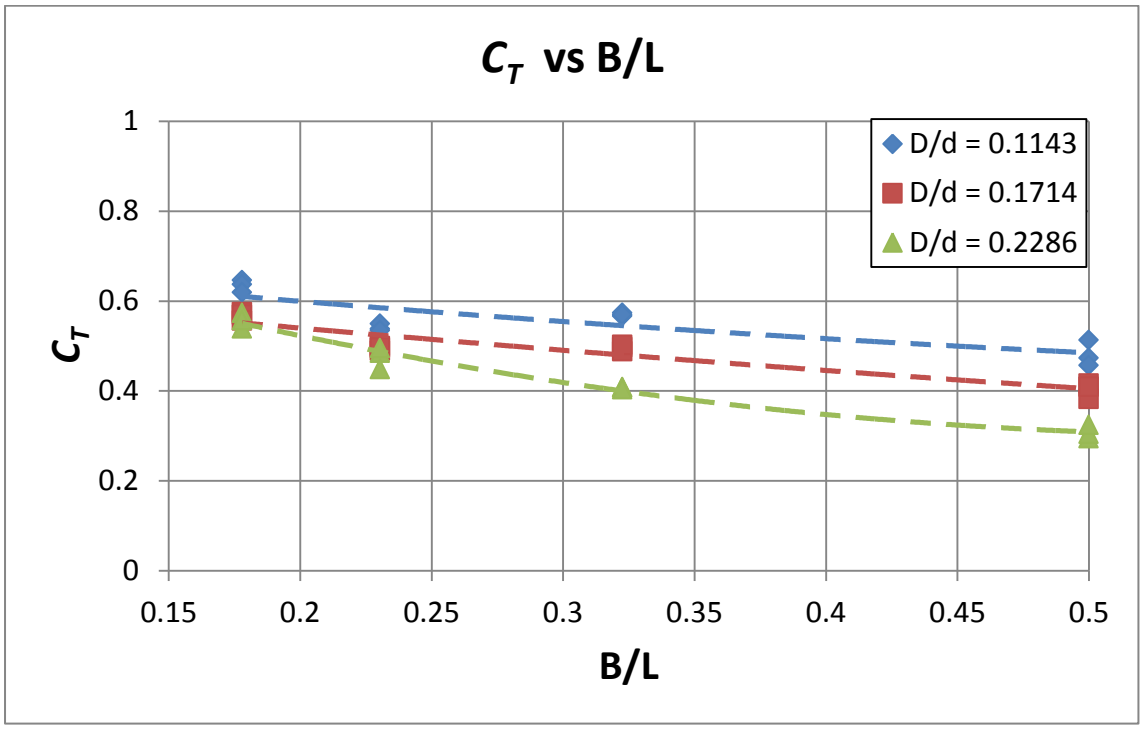

Figure 4.8: C_T vs. *B/L* of random waves

It is found that the C_T recorded are relatively small ($C_t \leq 0.5$), which indicates that at least 50% attenuation of wave height was attained by H-type floating breakwater in irregular waves. The C_T reduces as *D/d* increases from 0.1143 to 0.2286. The lowest C_T values recorded is 0.3 for *D/d* = 0.2286 at *B/L=0.5*. The figure also demonstrate a decrease of C_T with an increase in *B/L*, indicating that the

breakwater restricts wave transmission more effectively in seas dominated by shorter period waves.

The variation of C_T with respect to D/d is remarkably (about 10%) at B/L > 0.3 whilst the variation at B/L < 0.3 is relatively small (about 5%). This implies that the optimum wave attenuation performance of the H-type floating breakwater would be anticipated in shorter period waves.

The summary of C_T for irregular waves is presented in Table 4.4. In summary, the H-type floating breakwater can be regarded as a reasonably good wave attenuator, especially when adopted at sites exposed to shorter period waves.

Table 4.4: C_T ranges at D/d = 0.1143, 0.1714 and 0.2286

D/d	**0.1134**	**0.1714**	**0.2286**
C_T range	0.45 – 0.64	0.38– 0.57	0.29– 0.57
***Average* C_T**	0.56	0.49	0.44

4.5.1.2 WAVE REFLECTION

Wave reflection performance of the H-type floating breakwater is quantified by the wave reflection coefficient, C_R. The higher the C_R values, the greater will be the wave reflection effect. Figure 4.9 present the relationship between C_R and B/L at D/d = 0.1143, 0.1714 and 0.2286 in random waves.

It is learnt that the C_R plots of D/d = 0.1143, 0.1714 and 0.2286 are overlapping at 0.18 < B/L < 0.3. This indicates that the reflective performance of the H-type floating breakwater is not much affected by the change of breakwater draft when exposed to longer period waves. Nevertheless, the C_R in this B/L range is strongly governed by the change of wave length (or wave period) as seen in the figure, i.e. the higher the B/L, the higher the C_R values regardless of D/d.

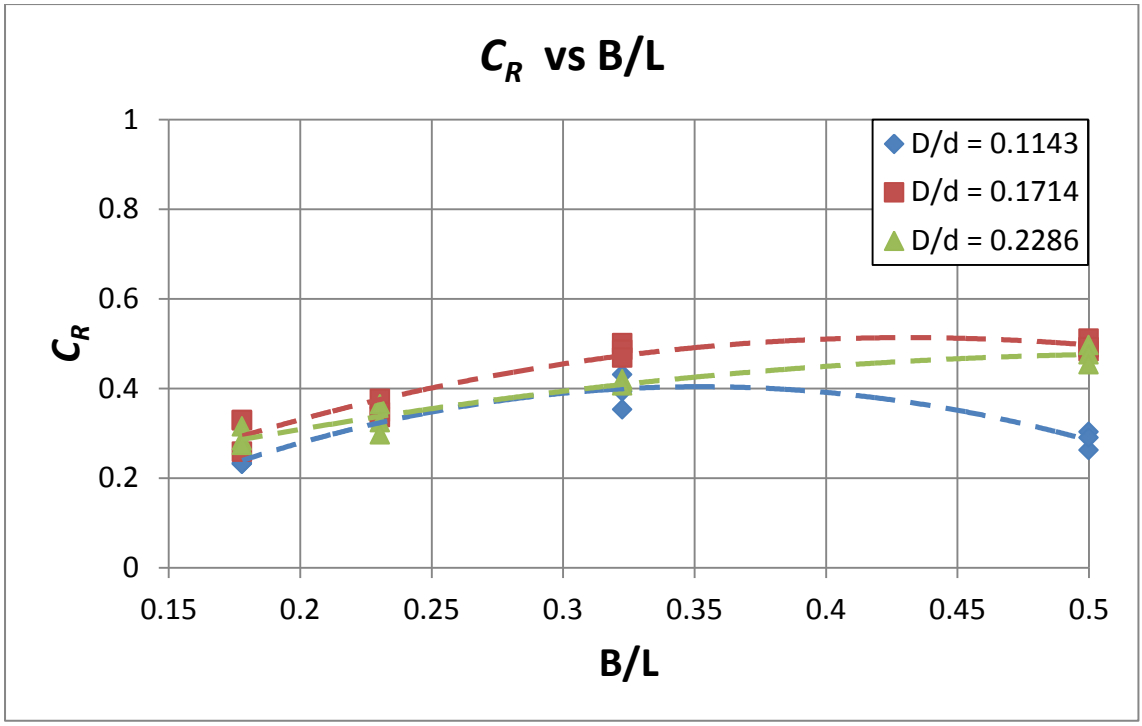

Figure 4.9: C_R vs. B/L of random waves

As B/L > 0.3, it is surprising to notice that the C_R of D/d = 0.1714 strike the highest values (C_R = 0.5). This is principally attributed to the fact that the breakwater immersed at D/d = 0.1714 provides the largest effective freeboard and draft for wave interception, resulting in high wave reflection. The C_R of higher relative breakwater draft (D/d = 0.2286) achieves the highest value at about 0.45. This observation is sensible because the shallow freeboard of the breakwater permits more wave overtopping to take place at the upper column of the water, which in turn reduces the amount of wave reflection. As expected, the breakwater with shallow draft (D/d = 0.1143) provides the least C_R (about 0.3) due to the allowance of transmission of large amount of wave energy beneath the breakwater.

Questions may arise if the H-type floating breakwater is a good anti-reflection coastal structure. To answer the question, let's take at the highest C_R value attained by the breakwater based on the experimental results. It is clear from the figure that the highest C_R recorded is about 0.5 at D/d = 0.1714. This is equivalent to 25% of the incident wave energy get reflected by the breakwater. This amount of reflected waves is relatively small as compared to the reflection caused by the bottom-mounted breakwaters, or even some of the floating breakwaters commercialized in the past decades.

The ranges of C_R for D/d = 0.1143, 0.1714 and 0.2286 in random waves are summarized in Table 4.5. In short, the H-type floating breakwater is a good anti-reflection structure and is considered suitable to be adopted as wave defense structure at marinas and fishing ports.

Table 4.5: C_R ranges at D/d = 0.1143, 0.1714 and 0.2286

D/d	**0.1134**	**0.1714**	**0.2286**
C_R range	0.23 – 0.43	0.25– 0.51	0.27– 0.49
***Average* C_R**	0.31	0.41	0.38

4.5.1.3 ENERGY DISSIPATION

Wave energy dissipation of the H-type floating breakwater is quantified by the energy loss/dissipation coefficient, C_L. The amount of energy loss due to the test model is reflected by the C_L^2 values. The higher the C_L^2 values, the greater will be the energy loss triggered by the H-type floating breakwater. The mechanisms identified to trigger energy loss are wave breaking, wave run-up and run down, formation of eddies underneath the test model, sound and heat. Since these phenomena are difficult to be measured physically, the loss of energy is often quantified based on the Principle of Conservation of Energy which is presented in Section 2.1.6. Figure 4.10 present the C_L^2 of the H-type floating breakwater plotted against B/L at D/d = 0.1143, 0.1714 and 0.2285 in random waves.

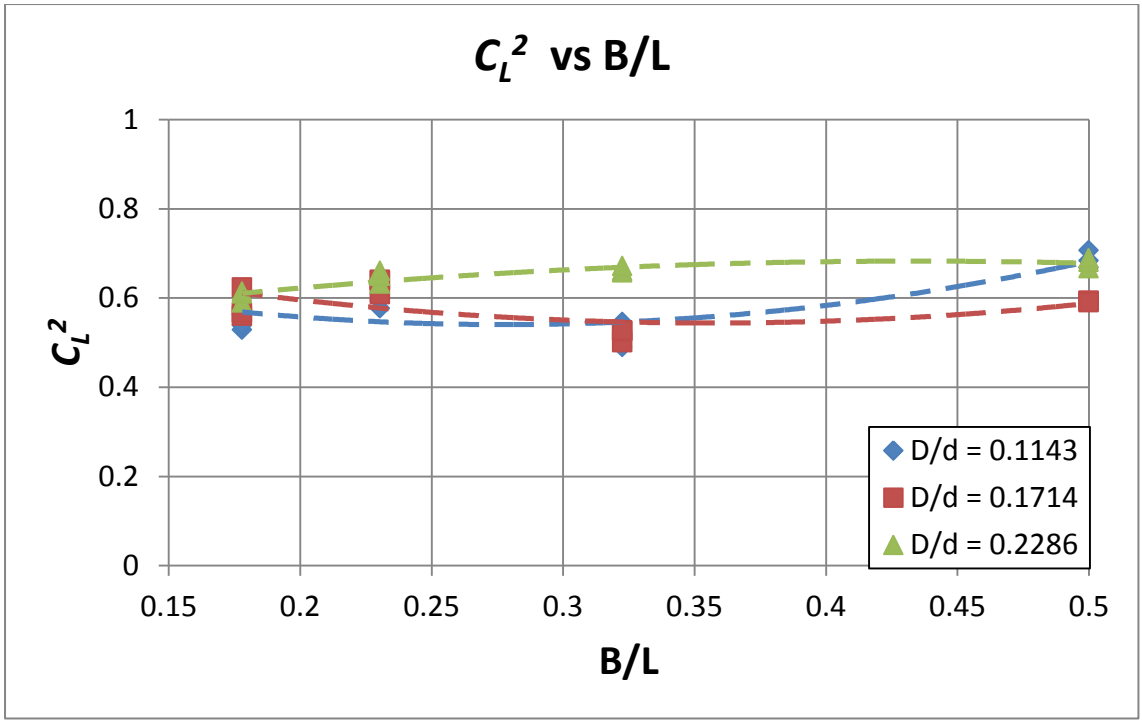

Figure 4.10: C_L^2 vs. *B/L* of random waves

It is observed from the figure that the C_L^2 of the test models of different *D/d* do not alter much as *B/L* increases. It can be concluded that the C_L^2 of the test models with 0.1143 < *D/d* < 0.2286 are not sensitive to the change of wave period. The range and average values of C_L^2 are summarized in Table 4.6. These C_L values are regarded to be in higher range, suggesting that that the configuration of the H-type floating breakwater is helpful in dissipating energy of waves of different periods. It is indeed a good energy dissipater especially when it is deeply immersed.

Table 4.6: C_L^2 ranges at *D/d* = 0.1143, 0.1714 and 0.2286

D/d	**0.1134**	**0.1714**	**0.2286**
C_L^2 range	0.49 – 0.70	0.50– 0.64	0.58– 0.68
***Average* C_L^2**	0.59	0.58	0.64

4.5.2 EFFECT OF WAVE PARAMETER

In this study, the energy coefficients of the H-type floating breakwater are also plotted with a dimensionless wave steepness parameter H_i/gT_p^2 where H_i is the incident significant wave height (equivalent to H_{m0}), g is the acceleration of gravity and T_p is the peak wave period. H_i/gT_p^2 is also one of the most commonly used parameters in the design of coastal structures. Similarly, the C_T, C_R and C_L are plotted against H_i/gT_p^2 in Figures 4.11 – 4.13.

4.5.2.1 WAVE TRANSMISSION

Figure 4.11 shows the relationship between C_T and H_i/gT_p^2 for D/d = 0.1143, 0.1714 and 0.2286. The C_T data for the respective D/d spreads over the range of H_i/gT_p^2 with unnoticed variations. This proves that the wave attenuation performance of the H-type floating breakwater is less controlled by the steepness of waves. Nevertheless, it is seen from the figure that the C_T is more influenced by D/d. The means of C_T for D/d = 0.1143, 0.1714 and 0.2286 are 0.55, 0.48 and 0.40, respectively.

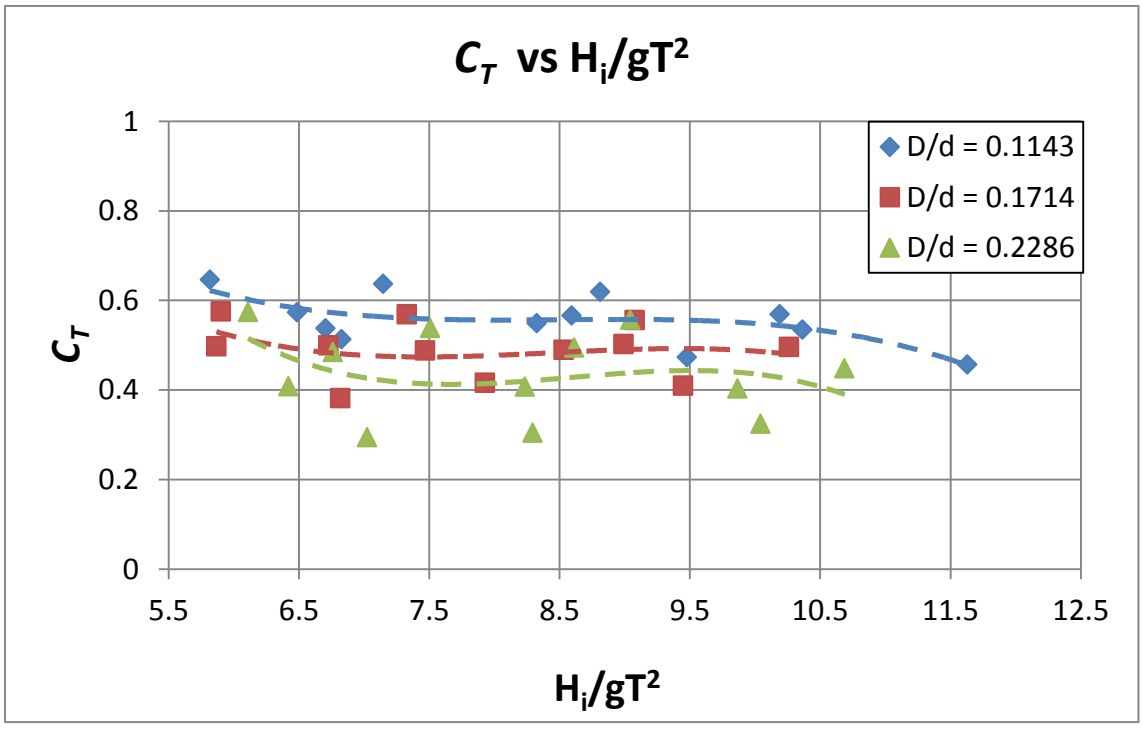

Figure 4.11: C_T vs. $\frac{H_i}{gT^2}$ of random waves

4.5.2.2 WAVE REFLECTION

The response of C_R with respect to H_i/gT_p^2 is presented in Figure 4.12. The C_R data are rather scattered when plotted against H_i/gT_p^2 regardless of D/d. The general behaviors of C_R are graphically represented by best-fit plots for the ease of interpretation of results. It is apparent that H_i/gT_p^2 may not be a significant design parameter to the reflective characteristics of the H-type floating breakwater. In general, the means of C_R for D/d = 0.1143, 0.1714 and 0.2286 are 0.30, 0.40 and 0.35, respectively.

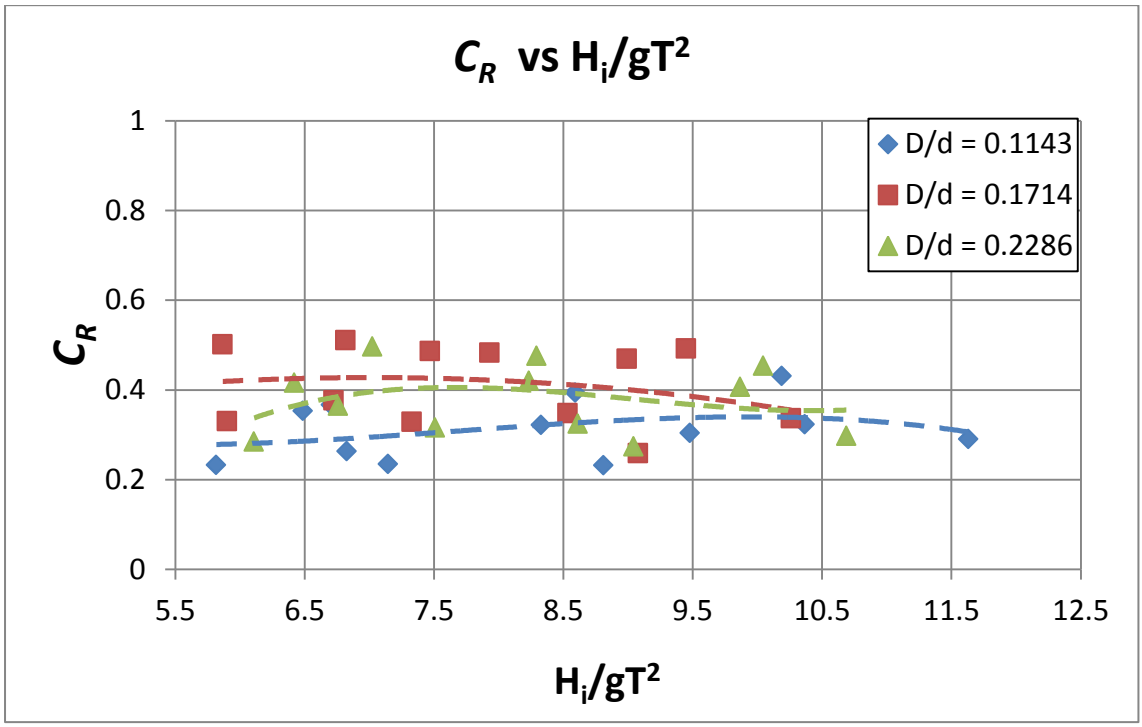

Figure 4.12: C_R vs. $\frac{H_i}{gT^2}$ of random waves

4.5.2.3 ENERGY DISSIPATION

The energy dissipation characteristic of the H-type floating breakwater with respect to the relative wave steepness parameter is shown in Figure 4.13. It is apparent that the C_L^2 for D/d = 0.1143, 0.1714 and 0.2286 are closely related to each other and ranges from 0.70 to 0.88. Similarly, H_i/gT_p^2 is not a governing parameter influencing C_L^2 within the tested D/d range.

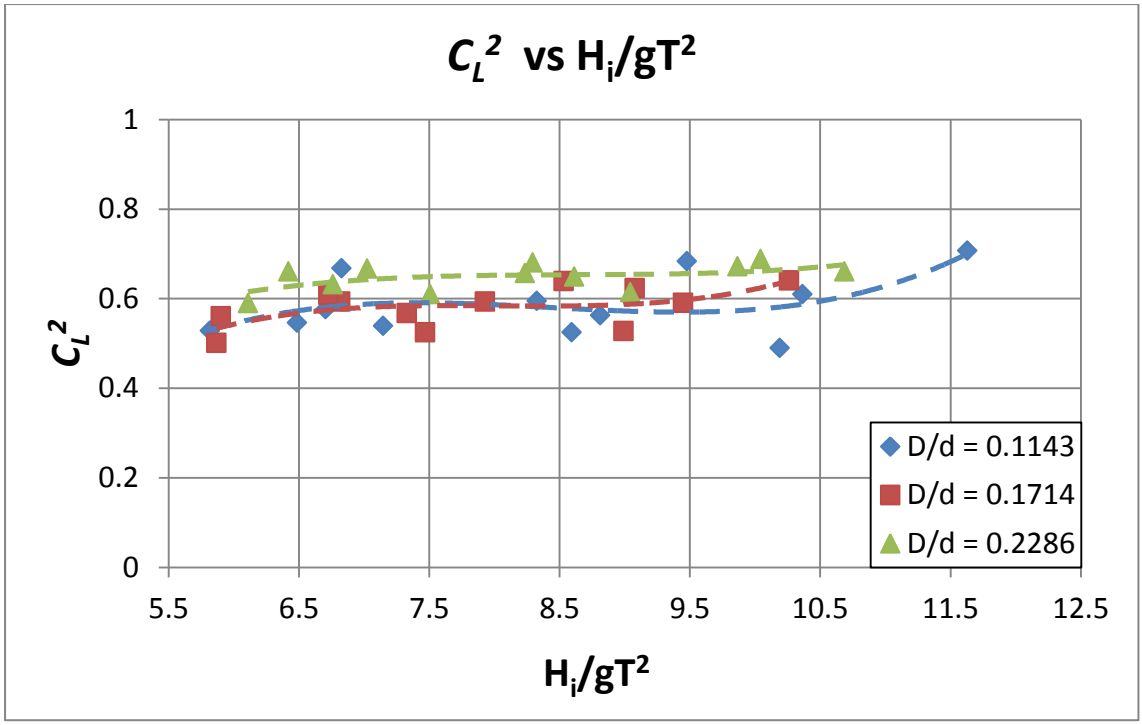

Figure 4.13: C_L^2 vs. $\frac{H_i}{gT^2}$ of random waves

4.5.2.4 SUMMARY OF WAVE STEEPNESS PARAMETER

In summary, the above results show that H_i/gT_p^2 is not a strong parameter influencing the energy coefficients. Hence, this parameter is suggested to be exempted when conducting the dimensional analysis for the energy coefficients of the H-type floating breakwater. It is stressed that the relative wave steepness parameter would not contribute significant effect to the change of energy coefficients of the breakwater for $0.1143 < D/d < 0.2286$.

4.6 COMPARISONS OF RESULTS

4.6.1 MODELS OF DIFFERENT SCALE FACTORS

It is worthwhile to compare the existing experimental results of the physical breakwater model of 1:10 with those of the model of 1:5 (Dexter, 2012). Note that the models of different scales were tested using similar test environment in the laboratory. The energy coefficients of both test models are demonstrated in Figures 4.14 – 4.16.

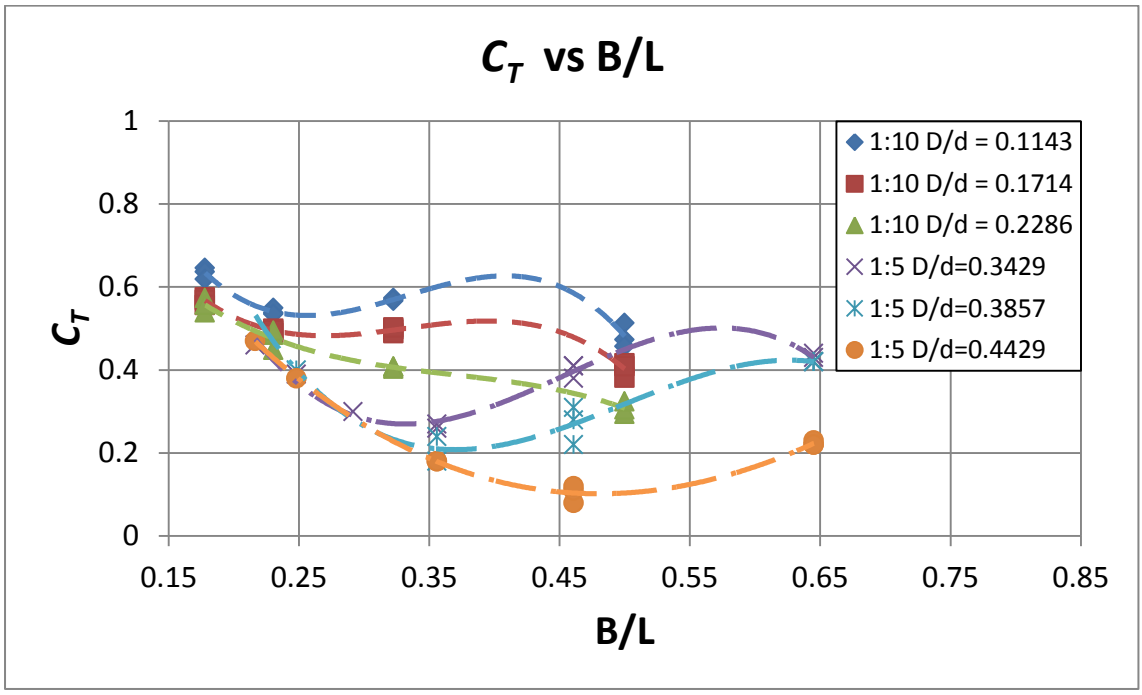

Figure 4.14: Comparison of C_T between models 1:10 and 1:5

In Figure 4.14, it is seen that the C_T of the 1:5 model is smaller than those of 1:10 model. Although larger models with higher *B/L* and *D/d* tend to restrict the transmission of wave energy more, they are massive structure and the construction cost may be higher. Larger structures with deeper immersion may be desirable for sites that require high level of wave tranquility. Smaller and cheaper breakwaters may be favorable to be used as barriers to provide perimeter protection to fishing ports and safe guarded swimming zones.

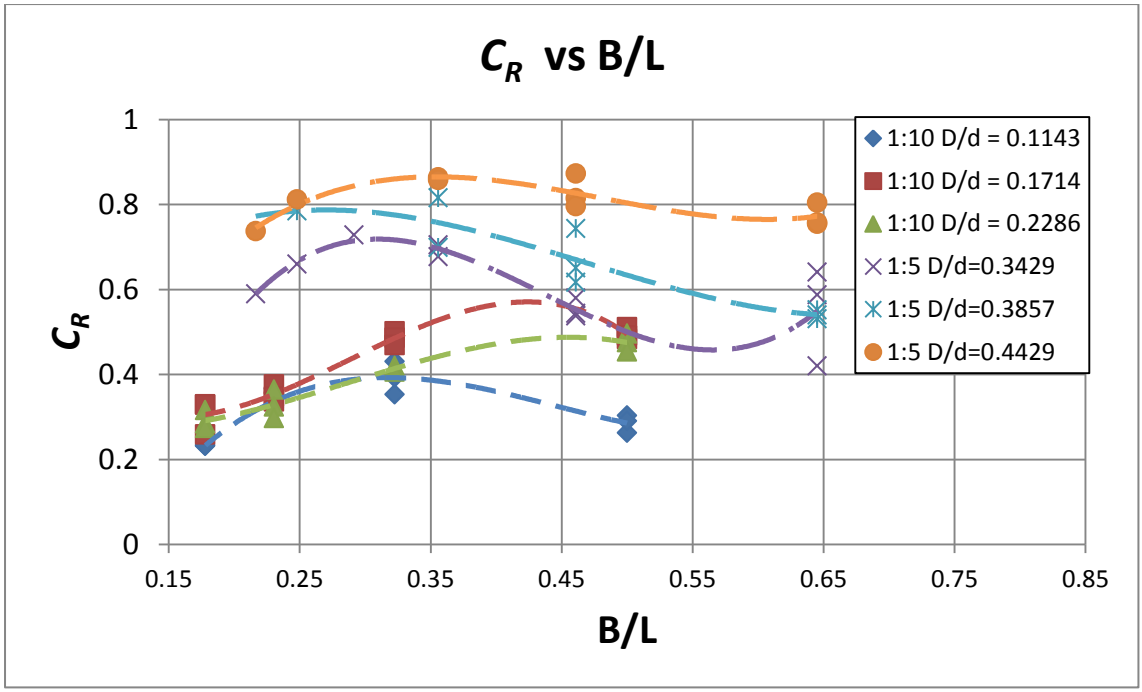

Figure 4.15: Comparison of C_R between models 1:10 and 1:5

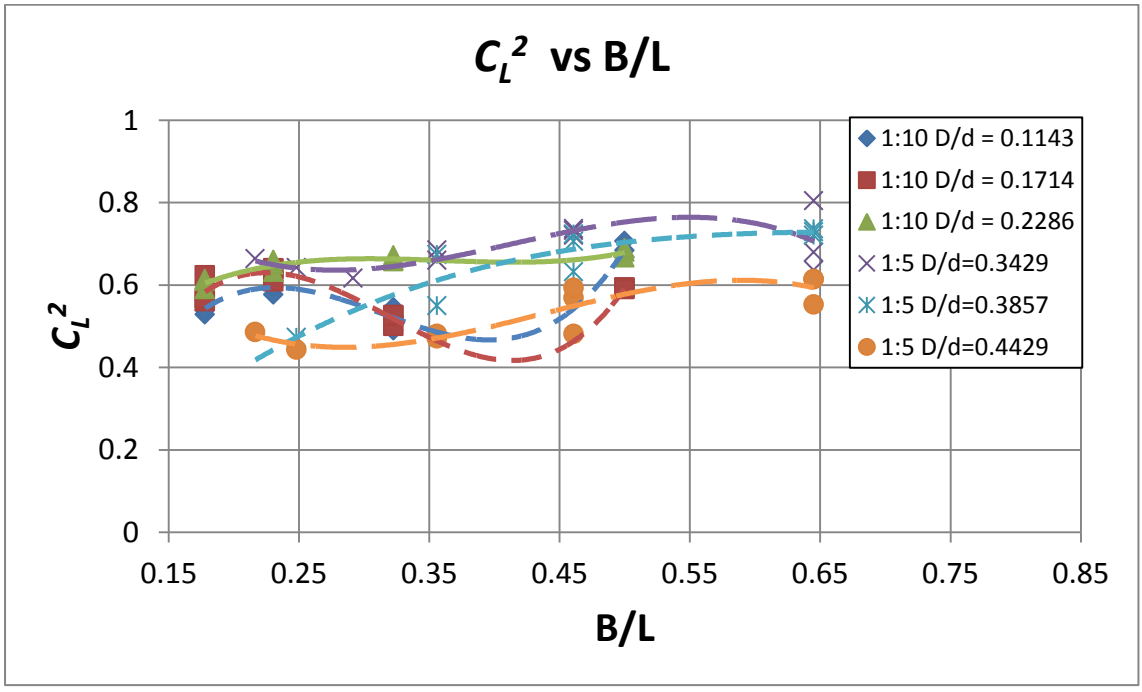

Figure 4.16: Comparison of C_L^2 between models 1:10 and 1:5

One of the major drawbacks of building a large floating breakwater is the wave reflection it poses. The reflection coefficients by the 1:5 model, as shown in Figure 4.15, are generally high due to their deep immersion in the water ($0.3429 > D/d > 0.4429$). The reflected waves amplified the height of the incident waves, causing confusing sea states right in front of the test model. When large breakwater is used at site, it is likely to cause navigation hazards to small floating vessels.

From Figure 4.16, it is learnt that the smaller breakwater seems to serve as a better energy dissipater than the larger one. This is mainly attributed to the fact that the smaller model has more intense interactions with the incoming waves, resulting energy dissipation through wave breaking, turbulence, etc. On the other hand, the same scale of incident waves are mostly intercepted by the large model by the means of reflection.

The notion of 'better breakwater' with regards to breakwater size generally differs between one and another. Essentially, the choice of breakwater is entirely subjected to the client's objective and requirement. If high level of wave attenuation is the key consideration and the implication of wave reflection is not a problem, the larger breakwater of higher relative breakwater draft is deemed to be appropriate. However, if the environmental concerns and initial cost are of priority, then the smaller breakwater is regarded as a better breakwater.

4.6.2 OTHER FLOATING BREAKWATERS

The hydraulic performances of the H-type floating breakwater is compared with those of other types of breakwater developed by other researchers, namely cage-type, pontoon-type, box-type, Y-frame type and other floating breakwaters as listed in Table 4.7. The comparison of C_T, C_R and C_L^2 are shown in Figures 4.17, 4.18 and 4.19 respectively. Note that these breakwaters were geometrically varied and were tested in different immersion depths and wave environments. Therefore, breakwater performance comparison can only be done qualitatively, and not quantitatively, in this study.

Table 4.7: Characteristics of other floating breakwater models that are compared against H-type floating breakwater in Figures 4.17 – 4.19.

Reference	Structure type	Dimension of model [m]	Experimental facilities [flume dimension & d in m]	Main parameters ranges	Hydrodynamics coefficients (C_t, C_r ,C_l)
Bruce L. McCartney (1985)	Box-type FBW (B = 12 FT)	B = 4.0, l = 29.7, h = 1.5, D = 1.1	Tested for Olympia Harbor, Washington, *d* = 7.6	H_i = 0.50-1.10, T=2.50-4.00	C_t = 0.42-0.88
Bruce L. McCartney (1985)	Box-type FBW (B = 16 FT)	B = 4.8, l = 29.7, h = 1.5, D = 1.1	Tested for Olympia Harbor, Washington, *d* = 7.6	H_i = 0.50-1.10, T=2.50-4.00	C_t = 0.39-0.89
Mani J.S. (1991)	Y-Frame FBW	B = 0.5, l = 0.2, 0.3, 0.4, h = 0.3, D = 0.16-0.46	30 x 2 x 1.5, *d* = 1.0	D/d =0.46, H_i/L = 0.01-0.10 B/L =0.095-0.224	C_t = 0.31-0.79
Murali K. and Mani J.S. (1997)	Cage FBW	B = 0.6, 0.8, 1.0, l = 0.2, 0.3, 0.4, h = 0.3, D = 0.36-0.56	30 x 2 x 1.5, *d* = 1.0	D/d=0.46 H_i/L = 0.01-0.10 B/L =0.12-0.60	C_t = 0.08-0.58
Behzad M. and Akbari M. (2007)	Moored Pontoon Type FBW	B = 0.72, D = 0.3-0.4	33 x 5.5 x 1.5, *d* = 1.0	D/d=0.14-0.23 H_i=0.20-1.20 B/L =0.20-2.20	C_t = 0.55-0.89
Wang H.Y. and Sun Z.C. (2010)	Porous FBW (Directional Mooring)	B=0.68, l=0.32, h=0.2, porosity=0.63,D=0.4-0.44	50 x 0.7 x 1.0, *d*=0.44	H_i = 0.06 T=0.60-1.40 B/L = 0.132-0.569	C_t = 0.10-0.94 C_r = 0.09-0.25 C_l = 0.40-0.99
Wang H.Y. and Sun Z.C. (2010)	Porous FBW (Directional Mooring)	B=0.68, l=0.32, h=0.2, porosity=0.63, D=0.4-0.42	50 x 0.7 x 1.0, *d*=0.44	H_i = 0.06 T=0.60-1.40 B/L = 0.132-0.569	C_t = 0.01-0.66 C_r = 0.09-0.28 C_l = 0.72-1.00
Fang He et al. (2012)	Rectangular FBW without pneumatic chambers	B=0.75, l=1.42, h=0.4, D=0.235	45 x 1.55 x 1.5, *d* = 0.7	H_i = 0.04 T=1.10-1.80 B/L = 0.186-0.404	C_t = 0.35-0.91 C_r = 0.39-0.55 C_l = 0.05-0.72
Fang He et al. (2012)	Rectangular FBW with pneumatic chambers	B=0.75, l=1.42, h=0.4, D=0.235	45 x 1.55 x 1.5, *d* = 0.45-0.90	H_i = 0.04 T=1.10-1.80 B/L = 0.187-0.430	C_t = 0.18-0.65 C_r = 0.15-0.72 C_l = 0.45-0.88
Teh H.M. and Nuzul I.M. (2012)	H-shape FBW	B=0.20, l=0.29, h=0.10, D=0.065	12 x 0.3 x 0.45, *d*=0.20-0.30	D/d=0.22-0.325 H_i/L = 0.025-0.125 B/L =0.10-0.50	C_t = 0.18-0.70
Nuzul I.M. (2012)	Improved H-shape FBW	B=0.20, l=0.30, h=0.10, D=0.05-0.103	10 x 0.3 x 0.45, *d*=0.20-0.30	D/d=0.17-0.52 H_i=0.005-0.075 B/L =0.10-0.50	C_t = 0.15-0.65
Dexter M. (2013)	H-type FBW 1:5	B=1.00, l=1.44, h=0.50, D=0.24-0.31	25 x 1.5 x 3.2, *d*=0.7	D/d=0.34-0.44 H_i/L = 0.04-0.07 B/L =0.22-0.65	C_t = 0.08-0.47 C_r = 0.73-0.87 C_l = 0.44-0.61
Mahadi N.N.A – Present Work (2013)	H-type FBW 1:10	B=0.5, l=1.44, h=0.25, D=0.16	25 x 1.5 x 3.2, *d*=0.7	D/d=0.2286 H_i/L = 0.04-0.06 B/L =0.178-0.5	C_t = 0.29-0.57 C_r = 0.27-0.49 C_l = 0.58-0.68

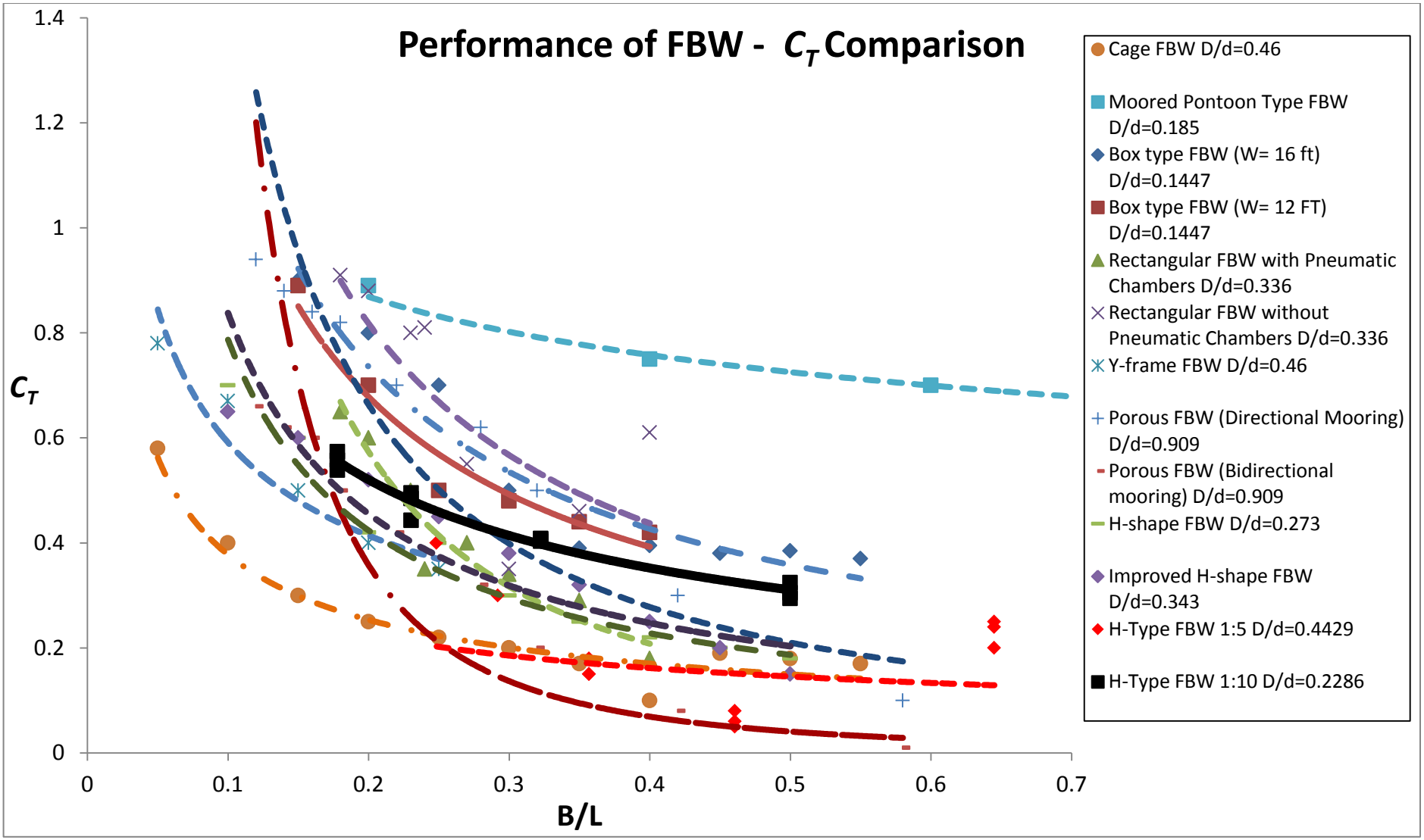

Figure 4.17: Comparison of Transmission Coefficient against other floating breakwaters

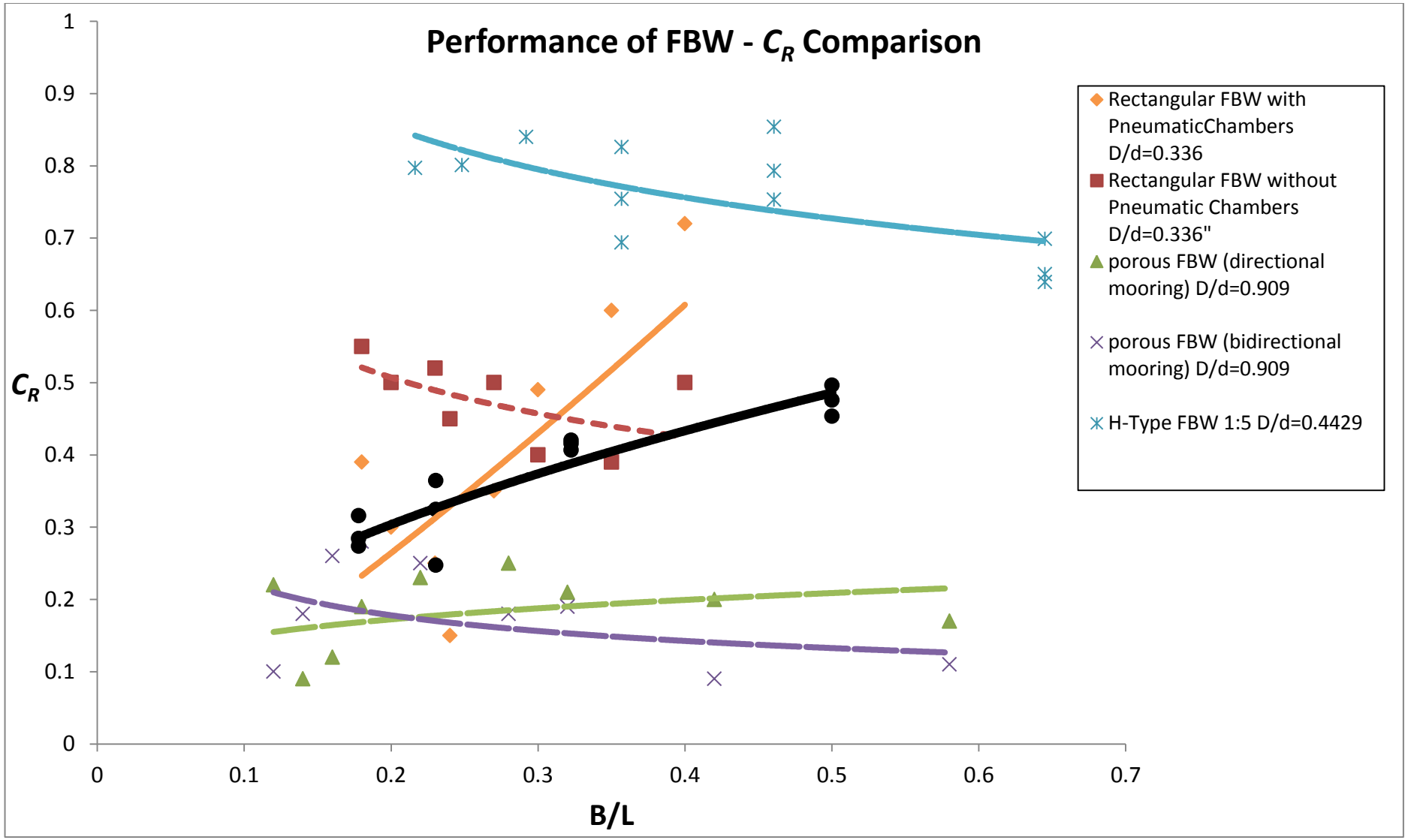

Figure 4.18: Comparison of Reflection Coefficient against other floating breakwaters

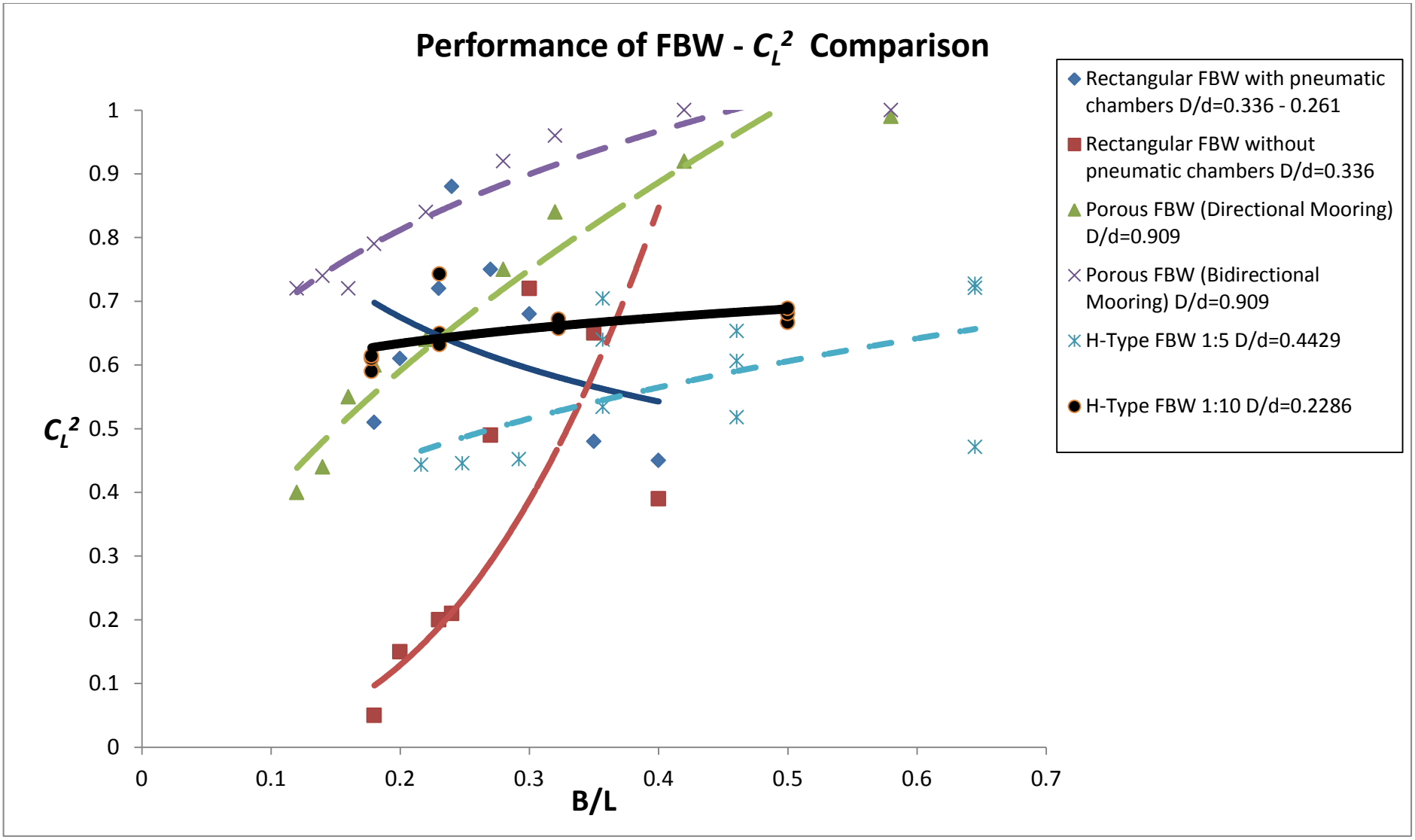

Figure 4.19: Comparison of Energy Dissipation against other floating breakwaters

Figure 4.17 shows the C_T of different types of floating breakwater corresponding to the relative breakwater width, *B/L*. The C_T of the H-type floating breakwater seems to follow the trend of other breakwaters, i.e. smaller C_T in larger *B/L* range. The breakwaters that achieve low C_T (i.e. cage-type, porous-type, Y-frame type, etc) have deeper drafts with *D/d* ranges from 0.44 to 0.91. Once again, it proves that the draft of the floating breakwater is the key factor affecting the wave attenuation of the floating breakwaters of various configurations.

The reflectivity of the floating breakwater is presented in Figure 4.18. There is no definite trend in the C_R variation corresponding to *B/L* because the amount of wave reflection is considerably controlled by the geometrical aspect of the breakwater. Porous breakwaters are the best anti-reflection structures because they permit the transmission of wave energy through the structures. Conversely, the more solid structure (e.g. the large H-type floating breakwater with 1:5) is a strong wave reflector. To minimize the reflective characteristics of the H-type floating breakwater, the overall size of the breakwater has to be reduced by half so as to bring down the C_R by about 40%.

The energy dissipative performances of the floating breakwaters are shown in Figure 4.19. It is clear that the H-type floating breakwater (1:10) is, over and above, an effective energy dissipater. It is seen from the figure that the porous breakwater is highly energy dissipative due to its deep draft with porous medium. The box-type breakwater is less energy dissipative due to the fact that the structure is lack of sharp edges for promotion of flow separation and turbulence.

CHAPTER 5

CONCLUSION AND RECOMMENDATIONS

This chapter concludes the overall finding of this study and the completion of objectives. Recommendations for future study are included to ease potential future researchers.

5.1 CONCLUSION

The wave attenuating ability and performance of 1:10 scale H-type floating breakwater was tested with regards to draft and varying wave condition. The key points of this study are listed below:

- H-type floating breakwater is a new design of floating breakwater. Previously tested models were of scale 1:20 (Teh and Nuzul, 2013) and 1:5 (Dexter, 2013) but with limited test cases.
- Breakwater dissipates wave energy through wave breaking, wave run-up and run-down, wave overtopping, wave reflection, wave transmission, wave dissipation, sound and heat.
- There are three physical modeling downscaling errors; model effects, measurement effects and scale effects. Through theoretical studies, scale effects are considered insignificant in this study.
- The water depth for this study was constant throughout the tests at 0.7 meter deep. The maximum wave height that can be generated and captured is roughly around 0.3 meter.
- The decomposition of reflected wave height and incident wave height was done according to Mansard and Funke's 3-point method. The spacing requirement between wave probes varies with wave period.
- Adjustment of the H-type floating breakwater draft was easily controlled by simply adding or removing weights in the ballast tank.

- Gain values are used as coefficients by wave generation program to generate specified wave height.
- The time series signal and frequency domain analysis of transmitted waves are considerably reduced when compared to the incident waves due to wave attenuation by the breakwater.
- Transmission coefficient analysis shows that more than 50% of wave energy was restricted by the model. The coefficient decreases with increasing relative breakwater width and shorter wave length. The transmission coefficient is reduced even further when the breakwater draft increases.
- Reflection coefficient analysis indicates that more wave energy was being reflected by the model when the relative breakwater width increases or as the wavelength shortens. It was also shown that low breakwater submergence results in low reflection of wave energy.
- Energy loss coefficient analysis reveals that the energy dissipation ability of breakwater is not sensitive to the changes in relative breakwater width or wave period. However, the energy dissipation does increase with deeper breakwater draft.
- Graphs of coefficients plotted against wave steepness parameter shows that the wave steepness has little to no effect on the overall attenuating ability of the breakwater.
- Comparison against similar model of larger scale 1:5 (Dexter, 2013) shows that the smaller breakwater model of 1:10 has higher transmission coefficient with lower reflective capability. However, the energy dissipation ability between the two models is roughly similar. Between the two models, the smaller scale of 1:10 is considered a good anti-reflective breakwater whereas the larger scale model of 1:5 is considered a reflective breakwater.
- Comparison with previous studies indicates that the 1:10 H-type breakwater model outperformed most breakwater models in term of energy dissipation with regards of having the lowest breakwater draft. The model is deemed to be highly effective considering the small scale of model and breakwater draft as compared to the rest of breakwater models.
- The effectiveness of the model increases with higher submergence of model or higher breakwater draft.

- The performance of H-type floating breakwater with scale of 1:10 is considered excellent and satisfactory. Further study with wider range of parameters will help in establishing the effectiveness of this breakwater design.

5.2 RECOMMENDATIONS

The H-type floating breakwater gave an overall satisfying performance in attenuating wave energy. These recommendations are meant to further improve the performance and effectiveness of the breakwater as well as to avoid potential errors during the experiments.

- Further tests should include wider range of parameters with different values of relative breakwater width and varying water depth.
- The fabrication of model should focus on sturdiness of model to prepare the model for testing against larger waves with higher strength and energy.
- The integrity of equipments such as mooring lines and hooks should be strengthened to give higher durability.
- Upgrading of equipments such as wave probes to overcome previous test limitations due to limited capabilities of equipments.
- Installation of shock absorbance material on the sides of the model to prevent damage from collision against the wall of wave flume.
- Further study on H-type breakwater model with focus on scale effects should be carried out to further validate the results of previous experiments.
- A study on the performance of H-type floating breakwater model with attached steel plate to increase breakwater draft can be compared to this research to study the effects of keel.

REFERENCES

Adee, B.H., 1976. A Review Of Developements And Problems In Using Floating Breakwaters. *Proceeding of 8th offshore technology conference*, 2, pp.225–236.

Andersen, T.L., Burcharth, H.F., Gironella, X. 2011. Comparison of new large and mall scale overtopping tests for rubble mound breakwaters. *Coastal Engineering* 58(4), pp. 351-373.

Bishop, C.T., 1982. Floating Tire Breakwater Comparison. *Journal of Waterway, Port, Coastal and Ocean Engineering*, 108(3), pp.421–426.

Blenkinsopp, C. and Chaplin, J. 2011. Void fraction measurements and scale effects in breaking waves in freshwater and seawater. *Coastal Engineering* 58(5), pp. 417-428.

Brebner, A.O. A. Ofuya, 1968. Floating Breakwaters. *Proceeding of the 5th Coastal Engineering Conference*, pp.1055–1085.

Chakrabarti, S. 1999. Wave interaction with an upright breakwater structure. *Ocean Engineering* 26, pp. 1003-1021.

Chanson, H., Aoki, S., Hoque, A. 2006. Scaling bubble entrainment and dispersion in vertical circular plunging jet flows: freshwater versus seawater. *Journal of Coastal Resources* 22(3), pp. 664-677.

Dexter, M. 2013. Wave Interactions of H-Type Floating Breakwater. *Final Year Project Civil Engineering.*

Dong, D.F. G.H. Zheng Y.N. Li Y.C. Teng B. Guan C.T. Lin, 2008. Experimentas On Wave Transmission Coefficient Of Floating Breakwaters. *Journal of Ocean Engineering*, 35, pp.931–938.

Falcao, A.., 2010. Wave Energy Utilization: A Review Of The Technologies. *Renewable sustainable energy*, 14(3), pp.899–918.

Franco, L., Geeraerts, J., Briganti, R., Willems, M., Bellotti, G., Rouck, J.D. 2009. Prototype measurements and small-scale model tests of wave overtopping at shallow rubble-mound breakwaters: the Ostia-Rome yacht harbour case. *Coastal Engineering* 56(2), pp. 154-165.

Geeraerts, J., Troch, P., Rouck, J.D., Verhaeghe, H., Bouma, J.J. 2007. Wave overtopping at coastal structures: prediction tools and related hazard analysis. *Journal of Cleaner Production* 15(16), pp. 1514-1521.

Guidelines and Specifications for Flood Hazard Mapping Partners. 2007. Wave runup and overtopping.

Hales, L.Z., 1981. *Floating Breakwater: State-of-the-art Literature Review, Technical Report No. 81-1*, U.S. Army, Corps of Engineers, Coastal Engineering Research Center.

He, A.W.-K. F. Huang Z. Law, 2013. An Experimental Study Of A Floating Breakwater With Asymetric Pneumatic Chambers For Wave Energy Extraction. *Journal of Applied Energy*, 106, pp.222–231.

Hughes, S.A. 1993. *Physical models and laboratory techniques in coastal engineering*, World Scientific Publishing Co. Pte. Ltd., Singapore.

Hedges, T.S. (n.d.). Wave breaking and reflection. Department of Civil Engineering, University of Liverpool.

Heller, V. 2011. Scale effects in physical hydraulic engineering models. *Journal of Hydraulic Research* 49(3), pp. 293-306.

Kobayashi, N. 1997. Wave runup and overtopping on beaches and coastal structures. *Research Report No. CACR-97-09*, pp. 1-48.

Loewen, M.R., O'Dor, M.A., Skafel, M.G. 1996. Bubbles entrained by mechanically generated breaking waves. *Journal of Geophysical Resources* 101, pp. 20759-20769.

Mani, C.R. J.S. Venugopal, 1987. Wave Transmission Characteristics Of Floating Berrier. *Proceeding of 2nd national conference on docks and harbours engineering*, pp.53–59.

Mani, J.., 1991. Design Of Y-frame Floating Breakwater. *Journal of Waterway, Port, Coastal and Ocean Engineering*, 117, pp.105–119.

Mansard, E. and Funke, E. 1980. The measurement of incident and reflected spectra using a least squares method. *Coastal Engineering Proceedings* 1(17).

McCartney, B.L., 1985. Floating Breakwater Design. *Journal of Waterway, Port, Coastal and Ocean Engineering*, 111, pp.304–317.

Murali, J.S. K. Mani, 1997. Performance Of Cage Floating Breakwater. *Journal of Waterway, Port, Coastal and Ocean Engineering*, pp.172–179.

Schüttrumpf, H. and Oumeraci, H. 2005. Scale and model effects in crest level design. *Proceedings of 2nd Coastal Symposium*, pp. 1-12.

Scott, J.C. 1975. The role of salt in whitecap persistence. *Journal of Deep Sea Resources* 22, pp. 653-657.

Slauenwhite, D.E., Johnson, B.D. 1996. The effect of organic matter on bubble surface tension in fresh water and sea water. *Journal of Geophysical Research 101*, pp. 3769-3744.

Tang, W.M. H.J. Hung C.C. Chen, 2011. Dynamics Of Dual Pontoon Floating Structure For Cage Aquaculture In A Two-dimensional Numerical Wave Tank. *Journal of Fluids and Structure*, 27, pp.918–936.

Teh, H.M. and Mohammed, N.I. 2012. Wave interactions with a floating breakwater. *Proceedings of the IEEE Colloquium on Humanities, Science and Engineering 2012.*

Tirindelli, M., Lamberti, A., Paphitis, D., Collins, M., Vidal, C., Hawkins, S., Moschella, P., Burcharth, H., Arcilla, A.S. 2000. *DELOS EVK3-CT-2000-00041*, pp. 1-53.

Vethamony, P., 1995. Wave Attenuation Characteristics of a Tethered Float system. *Journal of Ocean Engineering*, 22, pp.111–129.

Wang, Z.C. H.Y. Sun, 2010. Experimental Study Of A Porous Floating Breakwater. *Journal of Ocean Engineering*, 37, pp.520–527.

Williams, A.G. A.N. Abul-Azm, 1997. Breakwaters Floating Breakwater. *Journal of Ocean Engineering*, 24, pp.465–478.

Wu, J. 2000. Bubbles produced by breaking waves in fresh and salt waters: notes and correspondence. *Journal of Physical Ocean Engineering* 30, pp. 1809-1813.

Xie, Z. 2013. Two-phase flow modeling of spilling and plunging breaking waves. *Applied Mathematical Modeling* 37(6), pp. 3698-3713.